Development of M x N MIMO Detection Algorithm for 64 QAM using Sphere Decoding Algorithm

oŸk fMdkfMx rduhd dk mi;kx djr g, 64-QAM d fy, M x N MIMO [kkt dyu fof/k dk fodkl

BY
ANUP KUMAR KARDA

THESIS
MASTER OF TECHNOLOGY
IN
ELECTRONICS & COMMUNICATION ENGINEERING
(With Specialization in Communication Systems)

2014

DEPARTMENT OF ELECTRONICS & COMMUNICATION ENGINEERING

COLLEGE OF TECHNOLOGY AND ENGINEERING

MAHARANA PRATAP UNIVERSITY OF AGRICULTURE AND TECHNOLOGY

UDAIPUR-313001 (RAJASTHAN)

Development of M x N MIMO Detection Algorithm for 64 QAM using Sphere Decoding Algorithm

oYk fMdkfMx rduhd dk mi;kx djr g, 64-QAM d fy, M x N MIMO [kkt dyu fof/k dk fodkl

Thesis Submitted to the

MAHARANA PRATAP UNIVERSITY OF AGRICULTURE AND TECHNOLOGY

UDAIPUR

IN PARTIAL FULFILLMENT OF THE REQUIREMENT FOR
THE DEGREE OF

MASTER OF TECHNOLOGY

IN

ELECTRONICS & COMMUNICATION ENGINEERING

BY

ANUP KUMAR KARDA

2014

MAHARANA PRATAP UNIVERSITY OF AGRICULTURE AND TECHNOLOGY

COLLEGE OF TECHNOLOGY AND ENGINEERING, UDAIPUR

Dated:

CERTIFICATE – I

This is to certify that **Mr. Anup Kumar Karda** had successfully completed the comprehensive examination held on 31-01-2013 required under the regulations for the **Master of Technology** in **Electronics and Communication Engineering.**

Dr. Sunil Joshi

Professor & Head

Department of ECE

MAHARANA PRATAP UNIVERSITY OF AGRICULTURE AND TECHNOLOGY

COLLEGE OF TECHNOLOGY AND ENGINEERING, UDAIPUR

Dated:

CERTIFICATE – II

This is to certify that this thesis entitled **"Development of M x N MIMO Detection Algorithm for 64 QAM using Sphere Decoding Algorithm"** submitted for the degree of **Master of Technology** in the subject of **Electronics and Communication Engineering** embodies bonafide research work carried out by **Mr. Anup Kumar Karda** under my guidance and supervision and that no part of this thesis has been submitted for any other degree. The assistance and help received during the course of investigation has been fully acknowledged. The draft of the thesis was also approved by the advisory committee on 03/02/2014.

Dr. Sunil Joshi
Professor & Head
Department of ECE
C.T.A.E, Udaipur

Dr. Sunil Joshi
Major Advisor
C.T.A.E, Udaipur

Dr. B. P. Nandwana
Dean
C.T.A.E, Udaipur

MAHARANA PRATAP UNIVERSITY OF AGRICULTURE AND TECHNOLOGY

COLLEGE OF TECHNOLOGY AND ENGINEERING UDAIPUR

Dated:-

CERTIFICATE – III

This is to certify that this thesis entitled **"Development of M x N MIMO Detection Algorithm for 64 QAM using Sphere Decoding Algorithm"** submitted by **Mr. Anup Kumar Karda** to the Maharana Pratap University of Agriculture and Technology, Udaipur in the partial fulfillment of the requirement for the award of the degree of Master of Engineering in the subject of Electronics & Communication Engineering (Communication Systems) after recommendation by the external examiner was defended by the candidate before the following members of the examination committee. The performance of the candidate in the oral examination as satisfactory. We, therefore, recommend that the thesis be approved.

(Dr. Sunil Joshi)	**(Dr.Navneet Agarwal)**	**(Dr. Naveen Chaudhary)**
Major Advisor	Advisor	Advisor

(Dr. R.R. Joshi)

DRI Nominee

(Dr. Sunil Joshi)	**(Dr. N.S. Rathore)**
Professor and Head	Professor and Dean
ECE Department	C.T.A.E., Udaipur
C.T.A.E., Udaipur	

Approved

Director, Resident Instruction

MPUAT, Udaipur

MAHARANA PRATAP UNIVERSITY OF AGRICULTURE AND TECHNOLOGY

COLLEGE OF TECHNOLOGY AND ENGINEERING UDAIPUR

Dated:-

CERTIFICATE – IV

This is to certify that **Mr. Anup Kumar Karda** student of Master of Engineering Department of Electronics & Communication Engineering, College of Technology and Engineering has made all corrections/modifications in the thesis entitled **"Development of M x N MIMO Detection Algorithm for 64 QAM using Sphere Decoding Algorithm"** which was suggested by the external examiner and advisory committee in the oral examination held on 29-05-2014. The final copies of the thesis duly bound and corrected were submitted on……., are enclosed here with for approval.

(Dr. Sunil Joshi)

Major Advisor

(Dr. Sunil Joshi)

Professor and Head

Department of Electronics & Communication Engineering

C.T.A.E., Udaipur

(Dr. N.S. Rathore)

Professor and Dean

C.T.A.E., Udaipur

Abstract

A MIMO (Multiple Input Multiple Output) system employing multiple antennas at both the transmitter and the receiver is most suitable for high data rate communication as they enhance the capacity of a wireless link and has shown significant performance improvements in wireless communications. The major challenge being faced by such MIMO systems is at the receiver end. A tremendous amount of processing power is required on the receiver side as it involves detecting symbol from a complex signal.

MIMO detection techniques are broadly classified as linear, non-linear and exact detection methods. Linear methods like Zero-Forcing (ZF) offer low complexity with degraded Bit Error Rate (BER) performance as compared to non-linear methods like MMSE. Non-linear detectors are computationally not very expensive with acceptable performance. Exact solutions like Sphere Decoder provide optimal performance however it suffers from exponential complexity under certain conditions. The focus in this thesis is on Sphere Decoding algorithm and an effort has been made to develop a low complexity near-optimal MIMO detector. An optimal Maximum Likelihood (ML) detection using an exhaustive search method is chosen as reference.

In this work, firstly we investigate optimal search radius for sphere decoding algorithm. To find the optimal radius we use depth-first strategy. We consider the sphere radius to be valid only if the leaf nodes enclosed by it are more than the child nodes present. For sphere radius increasing from unity to a value, say n, we continue to simulate sphere decoder satisfying the above criteria of enclosing the leaf nodes. With the simulated results, an average value is calculated which becomes our optimal radius. We then use the same optimal search radius to implement 16-QAM, 32-QAM and 64-QAM for 2 x 2, 3 x 3 and 4 x 4 MIMO systems. These simulations will deliver near optimal performance with reasonably low complexity and improved BER.

Finally, we also investigate the performance of the sphere decoding algorithm for a fixed channel with conventional QR decomposition, Gram Schmitt orthogonalization, Household Transformation, Givens rotations and Sorted QD decomposition.

vu{ki.k

VklehVj vkj fjlhoj nkuk e ,dkf/kd ,Vuk MIMO ¼,dkf/kd buiV ,dkf/kd vkmViV½ i.kkyh e ,d ok;jyl fyd dh {kerk e of) d :i e mPp MkVk nj lpkj d fy, lcl mi;Dr g vkj ok;jyl lpkj e egRoi.k in'ku l/kkj fn[kkr gA bl MIMO flLVe d }kjk inf'kr dh tk jgh cMh pukrh fjlhoj vr e g] ;g ,d tfVy ldr l irhd dk irk yxku e 'kkfey gA ilLdj.k 'kfDr dk ,d tcjnLr jkf'k ikIrdrk dh vkj vko';d gA

MIMO irk yxku dh rduhd ekV rkj ij jf[kd] xj j[kh; vkj lVhd irk yxku d rjhd d :i e oxh—r fd;k tkrk gA thjk Qkjflx ¼ZF½ tl yhfu;j rjhdk l ?kVrh fcV ,jj jV nj (BER), MMSE tl xj j[kh; rjhdk dh ryuk d :i e in'ku d lkFk de tfVyrk inku djr gA xj j[kh; fMVDVjk dEl;V'kuyh Lohdk; in'ku d lkFk cgr egxk ugh gA ;g dN 'krk d rgr ?kkrh; tfVyrk l xLr g yfdu oŸk fMdkMj rjg lVhd lek/kku vudyre in'ku inku djr g] bl 'kk/k e Qkdl oŸk fMdkfMx ,YxkfjFe ij g vkj ,d i;kl ,d de tfVyrk d ikl b"Vre MIMO fMVDVj fodflr dju d fy, cuk;k x;k gA ,d foLrr [kkt fof/k dk mi;kx dj ,d b"Vre vf/kdre lHkkouk ¼ML½ dk irk yxku d lnHk d :i e puk tkrk gA

bl dke e] lcl igy ge oŸk fMdkfMx ,YxkfjFe d fy, b"Vre [kkt f=T;k tkp] ge xgjkb igy j.kuhfr dk mi;kx b"Vre f=T;k dk [kktu d fy, ge oŸk f=T;k d }kjk lyXu iRrh ukMl ekt n cPp ukMl dh ryuk e vf/kd g doy rHkh ekU; fd;k tkuk gA oŸk f=T;k ,d eY; d fy, ,drk l c<ku d fy,] n dk ekuk g] ge iRrh ukMl buDykflx dh mijkDr ekunMk dk lrk"ktud oŸk fMdkMj vudj.k dju d fy, tkjh gA flE;yVM ifj.kkek d lkFk ,d&,d vklr eY; gekj b"Vre f=T;k gk tkrk gA tk x.kuk dh g] ge 16-QAM, 32-QAM vkj 64-QAM 2 x 2 d fy,] 3 x 3 vkj 4 x 4 MIMO i.kkyh dk ykx dju d fy, gh b"Vre [kkt f=T;k dk mi;kx djA bu fley'ku dkQh de tfVyrk vkj cgrj fgV d lkFk b"Vre in'ku fudV forfjr djxA

vr e ge ijijkxr eY;kdu vi?kVu] xke f'eV] vkFkkxkuykbt'ku] ?kjy ifjoru] fxol ?keko vkj ble QR vi?kVu d lkFk ,d fuf'pr puy d fy, oŸk fMdkfMx ,YxkfjFke d in'ku dh tkp dj jg gA

CHAPTER 1
MIMO IN WIRELESS COMMUNICATION

1.1 Introduction

Multiple antennas at both transmitter and receiver end, in wireless systems, popularly known as MIMO (Multiple-Input Multiple-Output) systems, have rapidly gained popularity over the past decade due to its powerful performance-enhancing capabilities. Communication in wireless channels is impaired predominantly by multi-path fading. Multi-path is the arrival of the transmitted signal at an intended receiver through differing angles and/or differing time delays and/or differing frequency (i.e., Doppler) shifts due to the scattering of electromagnetic waves in the environment. Consequently, the received signal power fluctuates in space (due to angle spread) and/or frequency (due to delay spread) and/or time (due to Doppler spread) through the random superposition of the impinging multi-path components. This random fluctuation in signal level, known as fading, can severely affect the quality and reliability of wireless communication (Biglieri E., 2007). Additional constraints posed by limited power and scarce frequency bandwidth make the task of designing high data rate, high reliability wireless communication systems extremely challenging.

MIMO technology is a major breakthrough in wireless communication system design. This technology offers a number of benefits which helps in overcoming the challenges being posed by both the impairments in the wireless channel as well as resource constraints. In addition to the time and frequency dimensions that are exploited in conventional single-antenna (single-input single-output) wireless systems, the leverages of MIMO are realized by exploiting the spatial dimension (provided by the multiple antennas at the transmitter and the receiver).

1.2 Benefits of MIMO technology

Array gain, spatial diversity gain, spatial multiplexing gain and interference reduction are the benefits of MIMO technology that helps achieve significant performance gains. These gains are described in brief below.

1.2.1 Array gain

Array gain is the increase in the receiver SNR which results from the coherent combining effect of the wireless signals at a receiver. The coherent combining may be realized through spatial processing at the receive antenna array and/or spatial pre-processing at the transmit antenna array. Array gain improves resistance to noise, thereby improving the range and the coverage of a wireless network (Goldsmith A., 2005).

1.2.2 Spatial diversity gain

Spatial diversity gain mitigates fading. It is realized by providing the receiver with multiple (ideally independent) copies of the transmitted signal in space, frequency or time. With an increasing number of independent copies (referred to as the diversity order), the probability that at least one of the copies is not experiencing a deep fade increases, thereby improving the quality and reliability of reception (Biglieri E., 2007). A MIMO channel with N_T transmit antennas and N_R receive antennas potentially offers $N_T \times N_R$ independently fading links, and hence a spatial diversity order of $N_T \times N_R$.

1.2.3 Spatial multiplexing gain

MIMO systems offer transmitting multiple, independent data streams within the bandwidth of operation. Under suitable channel conditions, like rich scattering environment, the receiver can separate the data streams. The number of data streams that can be reliably supported by a MIMO channel equals the minimum of the number of transmit antennas and the number of receive antennas, i.e., min $\{N_T, N_R\}$ (Telatar I. E., 1999). Spatial multiplexing gain increases the capacity of a wireless network.

1.2.4 Interference reduction and avoidance

Multiple users sharing time and frequency resources lead to interference in wireless networks. Interference can be mitigated in MIMO systems by exploiting the spatial

dimension to increase the separation between users. In the presence of Interference, array gain increases the tolerance to noise as well as the interference power, hence improving the signal-to-noise-plus-interference ratio (SINR). Also spatial dimension helps in interference avoidance, i.e., directing signal energy towards the intended user and minimizing interference to other users. Interference reduction and avoidance improve the range and coverage of a wireless network.

1.3 Basic building blocks

The basic building blocks comprising a MIMO communication system is shown in figure 1.1. The information bits to be transmitted are encoded using convolution encoder and interleaved. The interleaved codeword is mapped to data symbols (like quadrature amplitude modulation or QAM symbols) by the symbol mapper. These data symbols are input to a space–time encoder that outputs one or more spatial data streams. The spatial data streams are then mapped to the transmit antennas by the space–time precoding block. The signals launched from the transmit antennas propagate through the channel and arrive at the receive antenna array (Biglieri E., 2007).. The receiver collects the signals at the output of each receive antenna element and reverses the transmitter operations in order to decode the data: receive space–time processing, followed by space–time decoding, symbol demapping, deinterleaving and decoding. Each of the building blocks offers the opportunity for significant design challenges and complexity–performance trade-offs.

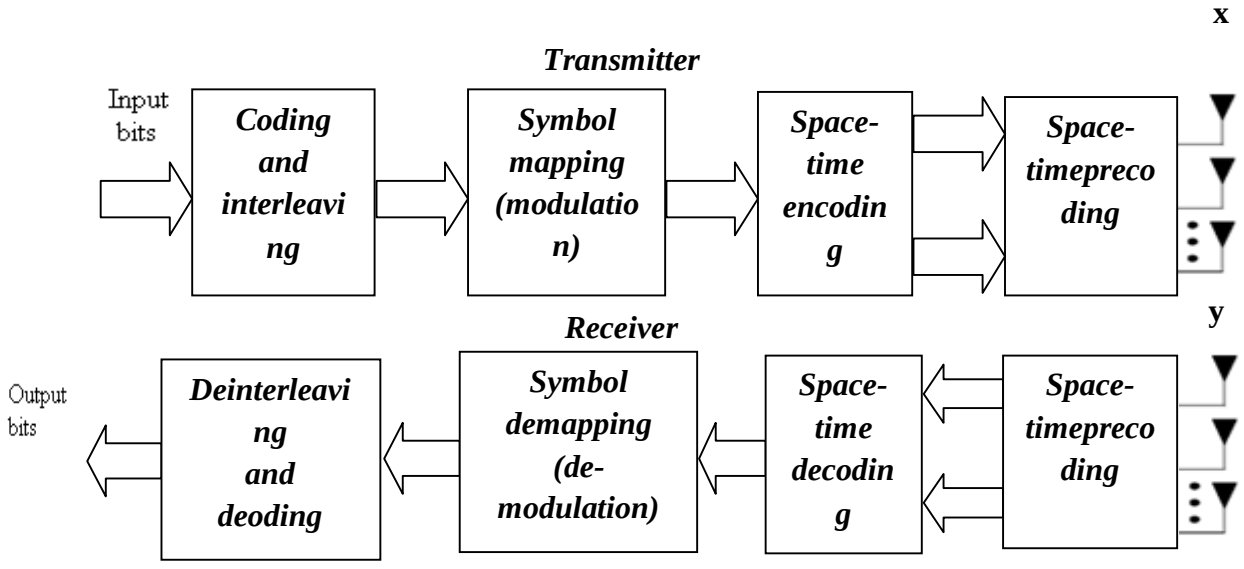

Figure 1.1: Diagram of a complex equivalent baseband MIMO communication system. xand y stand for the transmitted and received signal vectors respectively (Biglieri E., 2007).

1.4 MIMO channel and signal model

In a system with N_T transmit antennas and N_R receive antennas, assuming frequency-flat fading over the bandwidth of interest, the MIMO channel may be represented at a given time instant as an $N_T \times N_R$ matrix.

$$\boldsymbol{H} = \begin{bmatrix} \boldsymbol{H_{11}} & \boldsymbol{H_{12}} & \dots & \boldsymbol{H_{1N_T}} \\ \boldsymbol{H_{21}} & \boldsymbol{H_{22}} & \dots & \boldsymbol{H_{2N_T}} \\ \vdots & \vdots & \ddots & \vdots \\ \boldsymbol{H_{N_R1}} & \boldsymbol{H_{N_R2}} & \cdots & \boldsymbol{H_{N_RN_T}} \end{bmatrix} \tag{1.1}$$

where $H_{T,R}$ is the channel gain between the m^{th} receive and n^{th} transmit antenna pair. The n^{th} column of **H** is referred as the spatial signature of the n^{th} transmit antenna across the receive antenna array. The relative geometry of the N_T spatial signatures determines the distinguishability of the signals launched from the transmit antennas at a receiver (Biglieri E., 2007). For the case of single-input single-output channels, the individual channel gains comprising the MIMO channel are commonly modeled as zero-mean circularly symmetric complex Gaussian random variables. Consequently, the amplitudes $|H_{N,T}|$ are Rayleigh distributed random variables and the corresponding powers $|H_{N,T}|^2$ are exponentially distributed.

For the present work, we assumed that:

- The channel is rich in scattering which will provides us an ideal situation to implement MIMO.
- The channel matrix is random and the receiver has exact knowledge about the channel matrix entries.
- The channel is memoryless i.e. the channel is used independently for each and every time.
- The coefficient of the channel matrix are complex valued and normally disributed random variables while we take $|h_{ij}|$ to be Rayleigh distributed.

1.4.1 Independent & identically distributed (i.i.d.) Rayleigh fading channel

Considering an extreme condition were all antenna elements at the transmitter are collocated and likewise at the receiver. In such case, all the elements of **H** will be fully correlated and the spatial diversity order of the channel is one (Kermoal J. P., 2000).

Decorrelation between the channel elements will increase with antenna spacing. However, antenna spacing alone is not sufficient to ensure decorrelation. Rich (i.e., omni-directional and isotropic) scattering in the environment in combination with adequate antenna spacing ensures decorrelation of the MIMO channel elements. With rich scattering, the typical antenna spacing required for decorrelation is approximately $\lambda/2$, where λ is the wavelength corresponding to the frequency of operation. Under ideal conditions, when the channel elements are perfectly decorrelated, we have $H_{R,T}$ (N=1,2, ... ,N_R; T=1,2, ... ,N_T) ~ i.i.d. Summarizing, we get $\mathbf{H} = \mathbf{H_w}$, the classical i.i.d. frequency-flat Rayleigh fading MIMO channel. The spatial diversity order of $\mathbf{H_w}$ is $N_T \times N_R$.

1.4.2 Frequency-selective and time-selective fading

If the channel model assumes that the product of the bandwidth and the delay spread is very small then with increasing bandwidth and/or delay spread, the product is no longer negligible (0.1 is often considered the threshold for voice communication), resulting in channel realizations that are frequency-dependent, i.e., $\mathbf{H}(\mathbf{f})$ (Goldsmith A., 2005). The correlation properties in the frequency domain are a function of the power delay profile. The coherence bandwidth B_c can be defined as the minimum separation in bandwidth required to achieve decorrelation. For two frequencies f_1 and f_2 with $|f_1 - f_2| > B_c$, the coherence bandwidth is inversely proportional to the delay spread of the channel. Due to the motion of scatterers in the environment or of the transmitter or receiver, the channel realizations vary with time (Biglieri E., 2007). In frequency selective fading, coherence time T_c is defined as the minimum separation in time required for decorrelation of the

time-varying channel realizations. For two time instances t_1 and t_2 with $|t_1 - t_2| > T_c$, the coherence time is inversely proportional to the Doppler spread of the channel.

1.4.3 Real-world MIMO channels

In real world scenarios, the behavior of **H** can significantly deviate from $\mathbf{H_w}$ due to a combination of inadequate antenna spacing and/or inadequate scattering leading to spatial fading correlation. The presence of a fixed (i.e. line-of-sight) component in the channel will result in Ricean fading. These real-world MIMO channels are triply selective, i.e., they exhibit fading across space, time and frequency. In the presence of LOS component between the transmitter and the receiver, the MIMO channel can be modeled as the sum of a fixed component and a fading component (Goldsmith A., 2005)

$$\boldsymbol{H} = \sqrt{\frac{K}{1+K}}\,\overline{\boldsymbol{H}} + \sqrt{\frac{K}{1+K}}\,\boldsymbol{H_w} \tag{1.2}$$

where $\sqrt{\frac{K}{1+K}}\,\overline{\boldsymbol{H}} = \mathrm{E}[\mathbf{H}]$ is the LOS component of the channel and $\sqrt{\frac{K}{1+K}}\,\boldsymbol{H_w}$ is the fading component, assuming uncorrelated fading. $K \geq 0$ in (1.2) is the Ricean K-factor of the channel and is defined as the ratio of the power in the LOS component of the channel to the power in the fading component. When $K = 0$ we have pure Rayleigh fading. At the other extreme $K = \infty$ corresponds to a non-fading channel.

1.4.4 Discrete-time signal model

For a frequency-flat fading MIMO channel, the commonly used discrete-time input–output relation over a symbol period is given by (Biglieri E., 2007)

$$\boldsymbol{y} = \sqrt{\frac{E_x}{M_T}}\,\boldsymbol{H}\boldsymbol{x} + \boldsymbol{z} \tag{1.3}$$

where **y** is the $N_R \times 1$ received signal vector, **x** is the $N_T \times 1$ transmitted signal vector, **z** is additive temporally white complex Gaussian noise with $\mathbf{E[zz^H]} = \mathbf{N_0 I_{N_R}}$ and E_x is the total average energy available at the transmitter over a symbol period having removed losses due to propagation and shadowing. The total average transmitted power over a symbol period can be constrained by assuming that the covariance matrix of **x**, $\mathbf{R_{XX}}$=

$\mathbf{E[xx^H]}$ satisfies $\mathrm{Tr}(\mathbf{R_{XX}}) = N_T$. The ratio $\rho = \mathbf{E_x/N_0}$ equals the SNR per receive antenna. The channel is block fading, i.e., the channel remains constant over N consecutive symbol periods (determined by the coherence time) and then changes in an independent fashion to a new realization.

1.5 MIMO Channel Capacity

Shannon capacity gives the maximum data rate possible that can be transmitted through the channel with a very small probability of bit error. Channel capacity is related to the knowledge of the channel gain matrix at the transmitter and/or receiver. Channel gain matrix **H** can be assumed to be known at both transmitter and receiver; it is represented as channel side information at the transmitter (CSIT) and channel side information at the receiver (CSIR), respectively. For a static channel CSIR is typically assumed, since the channel gains can be obtained easily by sending a pilot sequence for channel estimation. When the feedback path is present then CSIR from the receiver can be transferred to the transmitter to have CSIT (Jafar S., 2005). When the channel is not known some distribution on the channel gain matrix must be assumed. The most common model for this distribution is a zero-mean spatially white model, where the entries of **H** are assumed as i.i.d. unit variance, zero mean, complex circularly symmetric Gaussian random variables.

Optimal detection of the transmitted symbol requires ML decoding, due to the cross-coupling between the possible transmitted symbols at the receivers. In a MIMO matrix channel, when the transmitter do have a perfect CSI the exhaustive ML detection is prohibitive even for small number of transmitters (Jafar S., 2005). Whereas, the detection complexity can be reduced under perfect CSIT conditions.

1.5.1 **Static Channels**

The capacity of a MIMO channel is an extension of the mutual information formula for a SISO channel to a matrix channel. The capacity is given in terms of the mutual information between **x** the input vector and **y** the output vector, represented as (Khan A. A., 2008)

$$C = \max_{p(x)} \boldsymbol{I}(\mathbf{X};\mathbf{Y}) = \max_{p(x)} [\boldsymbol{H}(\mathbf{Y}) - \boldsymbol{H}(\mathbf{Y}|\mathbf{X})] \quad (1.4)$$

Where $\boldsymbol{H(Y)}$ and $\boldsymbol{H(Y|X)}$ is the entropy in **y** and **y|x**. Maximizing the mutual information is similar to maximizing the entropy since the fixed entropy of noise **z** is not dependent on channel.

Maximizing the mutual information over $\boldsymbol{R_x}$which satisfy the power constraint yields the capacity of the MIMO channel as:

$$\boldsymbol{C = \max_{R_x:Tr(R_x)=\rho} B \log_2 \det [I_{N_R} + HR_xH^H]} \quad (1.5)$$

This optimization depends upon whether or not **H** is known at transmitter.

1.5.1.1 Perfect channel knowledge at transmitter

Parallel decomposition of MIMO channel assumes perfect channel knowledge at the transmitter and receiver. The capacity is equal to the accumulated capacity of the parallel channels. Using (1.5) and assuming perfect channel knowledge MIMO channel capacity can be expressed in power allocation $P_i$of the i^{th} parallel channel as (Jafar S., 2005)

$$\boldsymbol{C = \max_{\rho_i=\sum_i \ \rho_i \le \rho} \sum_i B \log_2 \left(1 + \frac{P_i \gamma_i}{P}\right)} \quad (1.6)$$

$\rho_i = P_i / \sigma_n^2$ and $\gamma_i = \sigma_i^2 P / \sigma_n^2$ is SNR of the i^{th} parallel channel with full power. This results into a water filling power allocation MIMO channel represented as (Jafar S., 2005)

$$\frac{P_i}{P} = \begin{cases} \frac{1}{\gamma_0} - \frac{1}{\gamma_i} \gamma_i \ge \gamma_0 \\ 0 \qquad \gamma_i < \gamma_0 \end{cases} \quad (1.7)$$

where γ_0 is cutoff value.

1.5.1.2 Channel unknown at transmitter

When the receiver only has channel knowledge, the transmitter will not be able to optimize its covariance structure across the antennas at the input. When **H** follows a ZMSW gain, the best strategy is to allocate equal power to each transmitter without any bias in terms of mean of **H**, this results in input covariance matrix as $\mathbf{R_x} = (\rho / \mathsf{M_t})\mathbf{I}_{\mathsf{M_t}}$. The mutual information of channel is maximized by this input covariance matrix. The mutual information for $\mathsf{N_T}$ transmit antennas and $\mathsf{N_R}$ receive antennas is represented as (Jafar S., 2005)

$$\boldsymbol{I = B \log_2 \det \left[I_{M_r} + \frac{\rho}{M_t} H H^H \right]} \quad (1.8)$$

The probability distribution of the singular values of channel **H** effect the average mutual information of a random matrix **H**. For static channels if the transmitter is ignorant of the channel's average mutual information it cannot control data transmit rate to enable accurate reception of data.

When N_T and N_R increase singular values of **H** distribution can be defined using central limit theorem as a constant mutual information for all possible channel coefficients. This constant mutual information can be used to derive MIMO channel capacity with uncorrelated fading channels.

1.5.2 Fading Channels

Under flat-fading MIMO systems matrix channel gains h_{ij} vary with time. The channel capacity is dependent on the knowledge of **H** at the transmitter and receiver. With no CSI available at the transmitter outage capacity is used to describe the MIMO channel capacity under any arbitrary realization of **H** (Jafar S., 2005). A detailed account on channel capacity is given below.

1.5.2.1 Perfect Channel Knowledge at Transmitter

The average of the channel capacities related with each channel realization under perfect CSIT and CSIR is as represented in (1.7) with optimal power allocation and is termed as ergodic capacity. When the power of each channel realization is equal to the average power constraint $\boldsymbol{P}$ the ergodic capacity is represented as (Jafar S., 2005)

$$\boldsymbol{C = E_H \left[\max_{\rho_i = \sum_i \ \rho_i \le \rho} \sum_i B \log_2 \left(1 + \frac{P_i \gamma_i}{P} \right) \right]} \quad (1.9)$$

When there are different powers for different channel realizations under the condition that the average power constraint over all the channel realizations, the ergodic capacity now becomes

$$\boldsymbol{C = \max_{\rho_H : E[\rho_H] = \rho} \left[\max_{R_x : Tr(R_x) = \rho_H} B \log_2 \det \left[I_{N_R} + H R_x H^H \right] \right]} \quad (1.10)$$

1.5.2.2 Channel unknown at Transmitter

In the scenario when the channel is time-varying and the channel **H** is not known at the transmitter but known at the receiver, a ZMSW distribution of **H** is assumed at the transmitter. Here the capacity can be defined as ergodic capacity and the outage capacity. Maximum rate transmission, averaged over all channel realizations based only on distribution of **H** is regarded as ergodic capacity. It is quantified as (Khan A. A., 2008)

$$\boldsymbol{C} = \mathbf{max}_{\boldsymbol{R_x}:\boldsymbol{T_r}(\boldsymbol{R_x})=\boldsymbol{\rho}} E_H\left[\boldsymbol{B}\,\mathbf{log_2}\,\mathbf{det}\,[\boldsymbol{I_{N_R}} + \boldsymbol{HR_xH^H}]\right] \quad (1.11)$$

For ZMSW model the transmit power is divided among Nt and symbols are transmitted independently the ergodic capacity becomes (Khan A. A., 2008)

$$\mathrm{C} = E_H\left[\mathrm{B}\log_2\det\left[\mathbf{I}_{\mathrm{N_r}} + \frac{\rho}{N_t}\boldsymbol{HH^H}\right]\right]\ \mathrm{bps/Hz} \quad (1.12)$$

When both transmitter and receivers increase, the capacity grows linearly with $\min(N_T,N_R)$. If receivers are increased and transmitters are kept fixed, the capacity increases logarithmically with receivers. If the receivers are fixed while the number of transmitters increases, the capacity saturates at some fixed value. Ergodic capacity has the multiplexing gain of $\min(N_T,N_R)$, this means that each 3-dB SNR leads to an increase of $\min(N_T,N_R)$ bps/Hz in spectral efficiency.

1.5.2.3 Channel unknown at Transmitter and Receiver

When the CSI is neither at transmitter nor at receiver the capacity increase with number of transmit, receive antennas is no more observed (Stridh R., 2000). In fading channels when channel is not known both at transmitters and receivers, data rate is not increased with the increase in the number of transmit antennas. Whereas, under correlated fading conditions the increase in transmitters does affect the channel capacity positively.

1.6 Different Modulation Schemes

Various modulation techniques can be employed to modulate the data to be transmitted. These modulation techniques involve linear modulation techniques, constant envelope modulation techniques, combined linear and constant modulation techniques, spread spectrum modulation techniques and orthogonal frequency division multiplexing modulation technique.

1.6.1 Linear Modulation Techniques

In linear modulation schemes the amplitude of the transmitted signal varies linearly with the modulating signal. Linear techniques are well suited for wireless communication system because of their spectral efficiency. A transmitted signal x(t) can be represented as follows in a linear modulation scheme (Lathi B. P. 1998).

$$x(t) = A[m_R(t)\cos(w_c t) - m_I(t)\sin(w_c t)] \quad (1.13)$$

where A is the amplitude of the modulated signal *m(t)* in general complex form, f_c is the carrier frequency. It is obvious from the above equation that the amplitude of the carrier depends linearly on the modulating signal. These linear techniques are bandwidth efficient however they need RF amplifiers for transmission which are not power efficient. When non-linear amplifiers are used these result in degrading the spectral efficiency of linear modulation techniques. Some of the linear modulation schemes are Binary Phase Shift Keying (BPSK), Differential Phase Shift Keying (DPSK), Quadrature Phase Shift Keying (QPSK) and Offset PSK (OPSK).

1.6.2 Constant Envelope Modulation Techniques

Constant envelope modulation techniques have significance as these modulations use Class C power efficient amplifiers which eliminate the presence of the side lobes and help reduce the spectral widening. Many practical radio systems use non-linear modulation methods in which the amplitude of the carrier remains same regardless of the changes in the modulating waveform (Lathi B. P. 1998). However, constant envelope techniques are less spectral efficient than linear modulation methods but are more power efficient. Few examples of these modulation techniques are Binary Frequency Shift Keying, Minimum Shift Keying and Gaussian Minimum Shift Keying, etc.

1.6.3 Combined Linear and Constant Envelope Modulation Techniques

Communication systems using modulations techniques which vary the amplitude and phase of the carriers provide more room to take data bits and lesser bandwidth. Variation of signal envelope and phase provides more degree of freedom to map the baseband data in more possible carriers. Modulation techniques using this two dimensional freedom are termed as M-ary modulation. Some of these techniques are discussed below.

1.6.3.1 M-ary Phase Shift Keying (M-PSK)

In M-PSK the carrier phase can take a phase shift of M possible values to represent the user data bits. The M-PSK modulated signal can be represented as (Lathi B. P. 1998)

$$x_j(t) = \sqrt{\frac{2E_x}{T_x}}\cos\left[w_c t + (j-1)\frac{2\pi}{M}\right] \qquad 0 \le t \le T_s \tag{1.14}$$

where the symbol period $T_x = bT_b$ and energy per symbol $E_x = bE_b$. $b = log_2 M$ bits per symbol and *j=1 to M*. Symbols are equally spaced at $\sqrt{E_x}$ centered at origin. 8-PSK constellation diagram shown in Figure 1.3 illustrates that M-PSK is a constant envelope modulation technique.

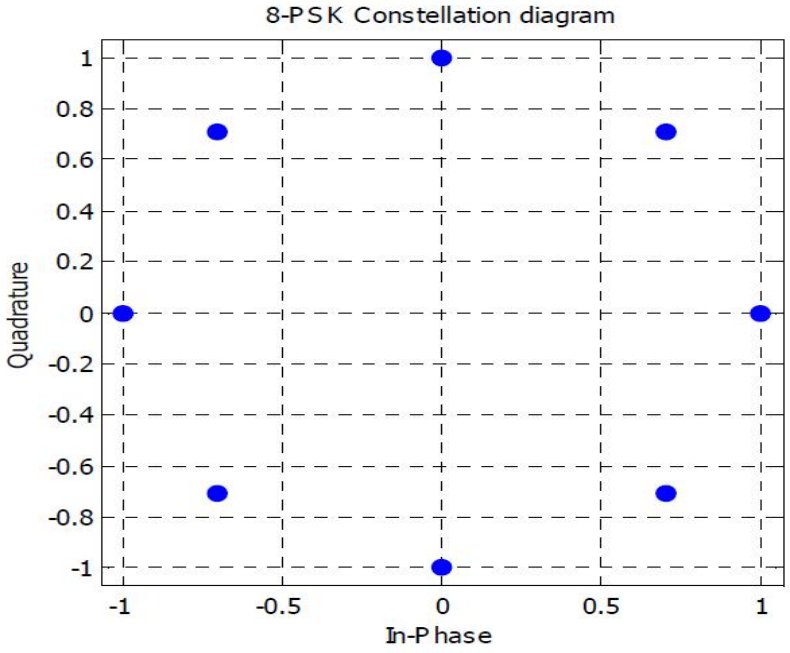

Figure 1.2: 8-PSK constellation (Lathi B. P. 1998)

1.6.3.2 Quadrature Amplitude Modulation (M-QAM)

For M-QAM, the information bits are encoded in both the amplitude and phase of the transmitted signal. Thus, whereas both M-PAM and M-PSK have one degree of freedom in which to encode the information bits (amplitude or phase); M-QAM has two degrees of freedom. As a result, M-QAM is more spectrally efficient than M-PAM and M-PSK, in that it can encode the most number of bits per symbol for a given average energy.

Figure 1.4 shows 16-QAM constellation. It's a square lattice representation of symbols. M-QAM signal can be expressed as (Lathi B. P. 1998)

$$x_i(t) = \sqrt{\frac{2E_{min}}{T_x}} a_i cos w_c t + \sqrt{\frac{2E_{min}}{T_x}} b_i cos w_c t \qquad 0 \leq t \leq T_s \qquad (1.15)$$

where i =1 to M, E_{min} is the minimum symbols energy with lowest amplitude. a_i and b_i represent the values of a particular signal point along x-axis and y-axis such that $x=a+jb$, representing the symbols location in the constellation.

M-QAM is power efficient than M-PSK. QAM is used in different applications, such as microwave digital radios, Digital Video Broadcasting Cable (DVB-C) systems, 3G cellular data-only systems, satellite communications etc

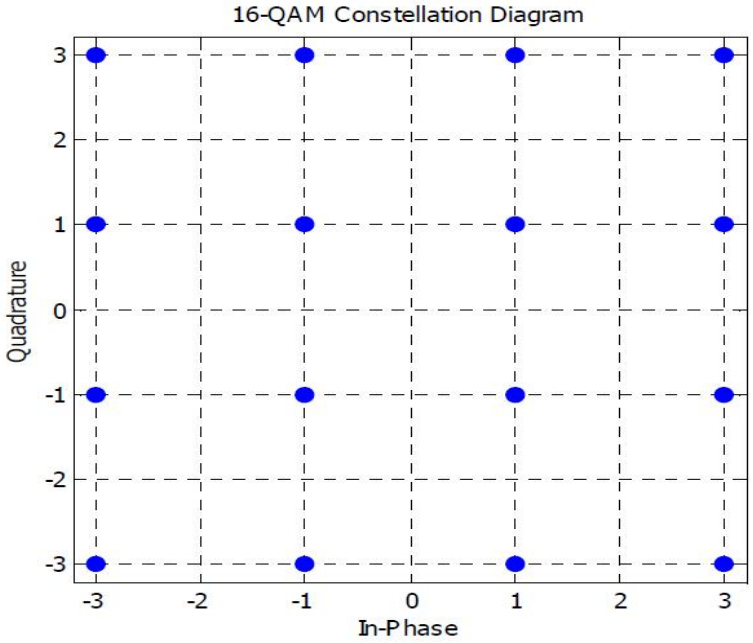

Figure 1.3: 16-QAM constellation diagram (Lathi B. P. 1998)

1.6.4 Spread Spectrum Modulation Techniques

Spread-spectrum is a means of transmission in which the signal occupies a bandwidth in excess of the minimum necessary to send the information; the band spread is accomplished by means of a code that is independent of the data, and a synchronized reception with the code at the receiver is used for despreading and subsequent data recovery.

Direct sequence spread spectrum (DS-SS) is employed in the IS-95 standard. In direct sequence code division multiple access (DS-CDMA) spreading codes like Walsh codes

and Pseudo-Noise (PN) sequence are used for channelization of users in forward and reverse link Their exists another form of spread spectrum called frequency-hopping spread spectrum(FH-SS) where the carrier frequency of the signal is moved (hopped) around in the band in a pseudorandom fashion (Rappaport T. S., 2009).

User data is multiplied with the spreading codes after encoding and interleaving. The spectrally expanded user's data is added and transmitted on to the channel. The channel induces noise, interferences in the transmitted signal. The received signal is despread using the corresponding codes to retrieve the original transmitted user data.

1.6.5 Orthogonal Frequency Division Multiplexing

Frequency division multiplexing (FDM) expands the concept of single carrier modulation by using multiple subcarriers within the same single channel. The total data rate to be sent in the channel is divided between the various subcarriers. Guard bands are generally introduced in between, so that the spectrum of subcarriers do not interfere with each other. OFDM extends the same concept and subcarriers are kept orthogonal to each other. The use of orthogonal subcarriers would allow the subcarriers' spectra to overlap, thus increasing the spectral efficiency. As long as orthogonality is maintained, it is possible to recover the individual subcarriers' signals despite their overlapping spectrums (Khan A. A., 2008). Due to its robustness in environments affected by high interference and multipath and to its spectral efficiency, orthogonal frequency-division multiplexing (OFDM) is considered as an effective modulation technique for high-speed digital transmissions.

OFDM is a multi-carrier modulation scheme where the carriers are orthogonal to each other. A single stream of digital data is split into several parallel streams of low data rate, each of the parallel stream then rides a carrier frequency within the original bandwidth such that all the carriers remain orthogonal to each other. The carriers are multiplexed to form a single OFDM carrier. It is also known as Multi-carrier modulation (MCM) or Discrete Multi Tone modulation (DMT).

1.7 MIMO Detection Problem

The task is to detect N_T transmitted symbols from a set of N_R observed symbols that have passed through a non-ideal communication channel, typically modeled as a linear system followed by an AWGN as shown in Figure1.4.

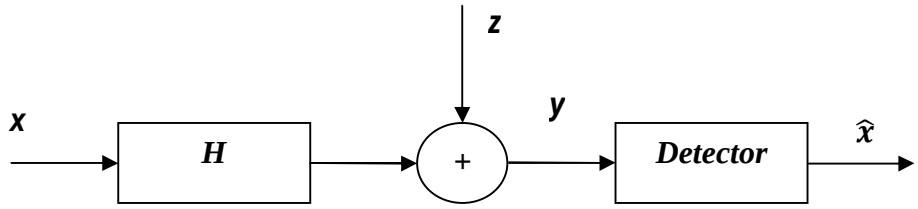

Figure 1.4: A simplified linear MIMO communication system showing the following discrete signals: transmitted symbol vector x, channel matrix H, additive noise vector z, receive vector y, and detected symbol vector$\hat{x}$.

Transmitted symbols form a known finite alphabet set of size C which are passed through the channel. The detector chooses one of the C^{N_T} possible transmitted symbol vectors from the available data. Assuming that the symbol vectors belonging to the alphabet set are equiprobable, the Maximum Likelihood (ML) detector always returns an optimal solution according to the following:

$$\hat{x} = \arg\max_{s \in C^{N_T}} P(\boldsymbol{y}\ is\ observed | \boldsymbol{x}\ was\ sent) \tag{1.25}$$

Assuming the additive noise **z** to be white and Gaussian, the ML detection problem of Figure 1.5 can be expressed as the minimization of the squared Euclidean distance to a target vector **y** over N_T dimensional finite discrete search set:

$$\hat{x} = \arg\min_{s \in C^{N_T}} \|\mathbf{y} - \mathbf{Hx}\|^2 \tag{1.26}$$

Optimal ML detection scheme needs to examine all C^{N_T}or 2^{bN_T}symbol combinations (b is the number of bits per symbol). The problem can be solved by enumerating over all possible **x** and finding the one that causes the minimum value as in (1.26).

In ML detection, optimization is performed over the space of all possible vectors **x**. Since the search space is discrete with **x** having integer components, this problem is posed in the literature as an integer least-squares optimization problem, and it belongs to the class of nondeterministic polynomial-time hard, NP-hard, combinatorial optimization problems (Khan A. A., 2008). A combinatorial optimization (CO) problem involves searching values for discrete variables in such a way an optimal solution with respect to a selected objective function is detected. A straight forward approach to the solution of a CO

problem would be exhaustive search, i.e. the enumeration of all possible solutions and choosing the one that minimizes the objective function in equation (1.26). A naive implementation of this search strategy results in a prohibitive complexity, as the number of candidate solutions increases exponentially with the problem size. Therefore, for a $N_T \times N_R$ MIMO system with symbols from M-QAM constellation alphabet the computational complexity increases exponentially with constellation size M and number of transmitters $N_T$as can be observed from (1.26).

This work focuses on designing MIMO detection algorithms capable of finding a near optimal solution with lesser than ML computational complexity. This will be a low complexity near optimal MIMO detector.

1.8 Organization of thesis

The rest of the thesis is organized as: Chapter 2 provides review of literature in detail. QR decomposition of channel matrix by Gram Schmitt orthogonalization, Household transformation, Givens rotation and sorted QR decomposition is elaborated in chapter 3. Chapter 4 deals with the various linear and non-linear detection algorithms along with sphere decoding algorithm and its modifications. Results and Discussions are quoted in chapter 5. The final chapter, chapter 6, summarizes/concludes the thesis.

CHAPTER 2
REWIEW OF LITERATURE

Chan Albert M. *et. al* (2002) presented a new sphere decoding algorithm which is even less computationally complex than the original sphere decoder. Moreover, the complexity of the new sphere decoder is relatively insensitive to the initial choice of sphere radius. Thus, by making the choice of radius sufficiently large, the ML solution is guaranteed with low complexity, even for large constellations.

Hassibi Babak *et. al* (2005) authors studied expected complexity, averaged over the noise and over the lattice. For the "sphere decoding" algorithm of Fincke and Pohst, they found a closed-form expression for the expected complexity, both for the infinite and finite lattice. They also demonstrated that for a wide range of signal-to-noise ratios (SNRs) and numbers of antennas, the expected complexity is polynomial, in fact, often roughly cubic. Since many communications systems operate at noise levels for which the expected complexity turns out to be polynomial, this suggested that maximum-likelihood decoding, which was hitherto thought to be computationally intractable, can, in fact, be implemented in real time—a result with many practical implications.

Myllylä Markus *et. al* (2005) a field programmable gate array (FPGA) implementation of a linear minimum mean square error (LMMSE) detector was considered for MIMO systems. Two square root free algorithms based on QR decomposition (QRD) were introduced for the implementation of LMMSE detector. Both algorithms were based on QRD via Givens rotations, namely coordinate rotation digital computer (CORDIC) and squared Givens rotation (SGR) algorithms. Linear and triangular shaped array architectures are considered to exploit the parallelism in the computations.

Two FPGA implementations of a LMMSE detector were considered based on the CORDIC and SGR algorithms for MIMO-OFDM systems, where the detector complexity and the number of required operations depend mainly of the number of subcarriers and the number of antennas. The detector architecture solutions were presented and compared for 2 × 2 and 4×4 antenna systems. A fast and parallel architecture was considered for lower dimensional systems, and a less complex architecture with easy scalability and time sharing PEs was considered for larger systems. The FPGA hardware implementations for both detectors were presented and the computational complexity of each implementation was evaluated and compared. The CORDIC based implementation was found to require more slices and less block multipliers compared to SGR based design. This is due to the normal arithmetic applied in the SGR algorithm and rotation based arithmetic applied in CORDIC algorithm. The SGR based detector was designed using the System Generator for DSP tool and the CORDIC based detector was designed using handwritten VHDL. The two design methods were compared during the work. It was noted that the System Generator based flow is useful especially if the designers are unexperienced with VHDL design.

Myllylä Markus *et. al* (2006) the complexity and performance of two novel list sphere detector (LSD) algorithms were studied and evaluated in multiple-input multiple-output orthogonal frequency division multiplexing (MIMO-OFDM) system. The LSDs were based on the K-best and the Schnorr-Euchner enumeration (SEE) algorithms. The required list sizes for LSD algorithms were determined for a 2×2 system with 4-quadrature amplitude modulation (QAM), 16-QAM, and 64-QAM. The complexity of the algorithms was compared by studying the number of visited nodes per received symbol vector by the algorithm in computer simulations.

The complexity and performance of two novel LSD algorithms, namely the SEE-LSD and the K-best-LSD, were evaluated and compared in MIMO-OFDM system. The needed list sizes were determined for 2 × 2 antenna system with 4-,16, and 64- QAM modulations. Also the average number of nodes visited by the algorithms were studied with the determined list sizes. The SEE-LSD algorithm was found to be less complex and feasible choice for implementation compared to the K-best based LSD algorithm.

Radosavljevic Predrag *et. al* (2006) proposed the design of soft sphere detection with the search method independently bounded for specific search levels (transmit antennas). The bounds are determined based on the distribution of the candidates found in each search level. The area and throughput estimates were compared against two previously implemented soft detectors. It was shown that the approach achieves significantly better performance than the previously implemented modified soft K-best solution mostly because no bound is established for the first search level. The proposed design was smaller and faster than other implemented list sphere detector with 256 search steps.

It is shown that the search process cannot be bounded for the first search level without a substantial performance loss. It is estimated that our solution is smaller than the previously implemented detectors and it achieves relatively high detection throughput with excellent performance. The search bounds are not fixed and can be easily adjusted based on the desired detection throughput and performance.

Azzam Luay *et. al* (2007) proposed a new structure for SD, which drastically reduces the overall complexity. The complexity was measured in terms of the floating point operations per second (FLOPS) and the number of nodes visited throughout the algorithm's tree search. This reduction in complexity was due to the ability of decoding the real and imaginary parts of every jointly detected symbol independently of each other, making use of the new lattice representation. They further showed by simulation results that the new approach achieves 80% reduction in the overall complexity compared to the conventional SD for a 2x2 system, and almost 50% reduction for the 4x4 and 6x6 cases, thus relaxing the requirements for hardware implementation.

Amiri Kiarash *et. al* (2008) suggested that K-best MIMO detection technique is the prominent method of simplifying the detection complexity in MIMO systems while maintaining BER performance comparable with the optimum maximum-likelihood (ML) detection technique. However, sorting the candidate nodes in the tree search of the conventional K-best detection can take a significant number of cycles which would reduce the achievable data rate of the detector. In order to reduce the delay, and keep high

performance at the same time, authors proposed using a novel sort-free based MIMO detector which avoided the demanding sorting step. Moreover, this detector utilized a novel modified real-valued decomposition (M-RVD) ordering that, when compared to the conventional real valued decomposition scheme, can improve the BER performance at no extra computational cost. They showed that proposed detector outperforms the conventional K-best detector with a smaller combination of computation and latency requirements.

For the BER simulations, the Rayleigh fading channel model was assumed, and the channel matrix was independent for each new transmission. The BER results of 4 × 4 and 3 × 3 systems were compared for a 16-QAM modulation scheme. In order to conduct a fair performance comparison, the *K* values were chosen such that the *K*-best technique has similar number of operations as that of the proposed sort-free scheme. The BER simulation results suggested that the proposed sort-free scheme can improve the BER performance more than 5 dB compared to the conventional *K*-best technique in higher SNR regimes.

Myllylä Markus *et. al* (2008) studied the effect of two sophisticated preprocessing methods, the channel matrix column ordering based on Euclidean norm and the sorted QR decomposition (SQRD), to the performance and complexity of the LSD algorithms and compared them to the traditional QR decomposition (QRD). They showed that the SQRD preprocessing is a simple way to decrease complexity of the LSD and it decreases the number of visited nodes approximately 20-30% compared to the QRD which results in significant number of saved arithmetic operations in the LSD. They also showed that the plain channel matrix column ordering is not feasible preprocessing method to be used with LSD in highly correlated channel realization.

The system was operating with 5 MHz bandwidth at a carrier frequency of 2.4 GHz. The K-best-LSD, the SEE-LSD, and the IR-LSD were considered for detection and an iterative max-log-MAP turbo decoder with 8 iterations was used for decoding. It illustrated the decrease in complexity of the number of additional multiplication (MUL) and addition (ADD) operations in preprocessing algorithms compared to traditional

QRD. It was seen that a significant number of operations are saved with the SQRD applied as preprocessing.

Stojnic Mihailo *et. al* (2008) targeted sphere decoding algorithm and attempted to find faster algorithms by pruning the search tree beyond what was done in the standard sphere decoding algorithm. The search tree is pruned by computing lower bounds on the optimal value of the objective function as the algorithm proceeds to descend down the search tree. They observed a tradeoff between the computational complexity required to compute a lower bound and the size of the pruned tree: the more effort they spend in computing a tight lower bound, the more branches that could be eliminated in the tree. Using ideas from semi-definite program (SDP)-duality theory and estimation theory, they proposed general frameworks for computing lower bounds on integer least squares problems. They proposed two families of algorithms, one that is appropriate for large problem dimensions and binary modulation, and the other that is appropriate for moderate-size dimensions yet high-order constellations. They then showed how in each case these bounds can be efficiently incorporated in the sphere decoding algorithm, often resulting in significant improvement of the expected complexity of solving the ML decoding problem, while maintaining the exact ML-performance.

Sun Yang *et. al* (2008) proposed a recursive Forward-Backward (F-B) trellis algorithm for soft-output MIMO detection. Instead of using the traditional tree topology, they represent the search space of the MIMO signals with a fully connected trellis and a Forward-Backward recursion was applied to compute the a posteriori probability (APP) for each coded data bit. The proposed detector had the following advantages: a) it kept a fixed throughput and had a regular datapath structure which made it amenable to VLSI implementation, and b) it attempted to maximize the a posteriori probability by tracing both forward and backward on the trellis and it always ensured that at least one candidate exists for every possible transmitted bit $x_k \in \{-1, +1\}$. Compared with the soft K-best detector, the proposed detector significantly reduced the complexity because sorting was not required, while still maintaining good performance.

Wu Jinhong *et. al* (2009) introduced a low complexity iterative soft output sphere decoding algorithm for coded transmissions over multiple antenna channels. Before the iterative detection and decoding starts, a modified hard decision sphere decoder produced a short (base) list of vectors with maximum likelihood metrics. In subsequent iterative soft detections, two competing lists with a small number of vectors were further generated for each coded bit, by utilizing the base list vectors and a priori information from the channel decoder. The corresponding likelihood metrics of the vectors in each competing list were combined to produce soft detection output that approximates the optimal maximum a posteriori (MAP) solution. The performance improved as the base list size increases and a short list can provide near-capacity performance after a few iterations. Compared with existing methods the proposed algorithm approaches the optimal performance better with significantly lower complexity requirements.

They tested the introduced algorithm in a 4 x 4 system. The information data were encoded by a half rate, memory 2 turbo code with interleaver length 576. The generator polynomial for each constituent encoder were (1,5/7*octal).* The coded 1152 bits were further interleaved before Graymapping into 16-QAM symbols. The QAM symbols were serial -to- parallel converted into 4-symbol vectors and transmitted.

Jeon Myeongwoon *et. al* (2009) proposed sphere decoding algorithms combined with other suboptimum detectors. Pre-estimated vectors by suboptimum detectors such as MMSE V-BLAST were used to assist sphere decoding algorithm. The number of search points in the tree search lattice area could be restricted, and the complexity can be reduced significantly. The number of limited constellation points can be changed by considering the trade-off between bit-error-rate (BER) performance and complexity. If the number of limited points according to SNR were adjusted, then the BER performance close to that of an optimal sphere decoding algorithm was achieved, and lower complexity than the Schnorr-Euchner algorithm.

Johannes Fink et. Al (2009) Sphere Decoding (SD) algorithms have been shown to provide maximum likelihood (ML) detection over Gaussian multiple input-multiple output (MIMO) channels with lower complexity than the exhaustive search. These

methods are based on a closest lattice point search over a limited search space (hypersphere). There exist several implementations of these algorithms pursuiting different search strategies and working either within a set of real numbers, thus called Real Sphere Decoders (RSD), or performing the search directly within a set of complex numbers, commonly known as Complex Sphere Decoders (CSD), so a performance comparison between the real and the complex version of the Schnorr-Euchner (SE) sphere decoder had been carried out by the authors in order to find out which algorithm is the most suitable depending on the application. Furthermore a recently appeared fixed-complexity version of the SE decoder (FSD) had been evaluated both in terms of complexity and performance and the results were compared with the original version. In contrast to yet existing complexity analyses, not only the number of visited nodes had been investigated but also the total number of operations.

Lee Jaeseok *et. al* (2010) presented a low-complexity list sphere search algorithm for achieving near-optimal a posteriori (APP) detection in iterative detection and decoding (IDD). Motivated by the fact that the list sphere decoding searching fixed number of lattice points is inefficient in many scenarios, they designed a criterion to search lattice points with non-vanishing likelihood and derived the optimal sphere radius satisfying this requirement. Through simulations on realistic IDD systems, they showed that the proposed method provides considerable complexity savings while maintaining near-optimal performance.

Ketonen Johanna *et. al* (2010) considered implementation of receivers for spatial multiplexing multiple-input multiple-output (MIMO) orthogonal-frequency division-multiplexing (OFDM) systems. The linear minimum mean-square error (LMMSE) and the k-best list sphere detector (LSD) were compared to the iterative successive interference cancellation (SIC) detector and the iterative k–best LSD. The performance of the algorithms were evaluated in 3G long-term evolution (LTE) system. The SIC algorithm was found to perform worse than the k-best LSD when the MIMO channels are highly correlated, while the performance difference diminished when the correlation decreased. The receivers were designed for 2x2 and 4x4 antenna systems and three

different modulation schemes. A modification to the k-best LSD which increased its detection rate was introduced. The SIC receiver had the best performance–complexity tradeoff in the 2x2 system but in the 4x4 case, the k-best LSD was the most efficient.

Eckert Sebastian *et. al* (2010) presented an algorithm and architecture of a soft-output sphere decoder with an optimized hardware implementation for 2x2 MIMO-OFDM reception. They introduced a novel table look-up approach for symbol enumeration that simplified the implementation of soft-output decoders. The HW implementation was targeted towards WLAN (IEEE 802.11n) with stringent latency and throughput requirements. Their implementation supported all modulation schemes (BPSK, QPSK, 16-QAM, 64-QAM) and showed near-optimal real-time performance.

Lei Sheng *et. al* (2010) conducted an adaptive control of the number of surviving branches for each of the single expansion (SE) stages in the original FSD (AC-FSD). In this controlling method, for each stage, the surviving branches were selected by a threshold value which was calculated from the minimum partial accumulated branch metric and the noise level. They compared the AC-FSD with the original FSD and a proposed simplified FSD (SFSD), and simulation results demonstrated that the AC-FSD with proper threshold can attain near-optimal performance with a much lower cost than that of the FSD and the SFSD when the system works in mid and high signal-to-noise ratio (SNR) regimes in practice.

Moon Sung-Hyun *et. al* (2010) proposed a new groupwise receive combiner design for multiple-input multiple-output spatial multiplexing systems. The conventional group detection (GD) suffers from a considerable performance loss since the noise components were not taken into account. The output signal-to-interference plus-noise ratio (SINR) was defined in each subgroup in order to consider both the desired signal and noise statistics. Adopting the real-valued representation, they provided an optimal receive combiner which maximized the SINR with a general group size. The simulation results showed that the proposed scheme achieves a large performance gain over the conventional GD in coded systems. Also, when combining with near-optimal detection

algorithms such as sphere decoder, the proposed GD scheme offered a comparable performance with significant reduced complexity.

Sun Yang *et. al* (2010) presented a novel low-complexity multiple-input multiple output (MIMO) detection scheme using a distributed M-algorithm (DM) to achieve high performance soft MIMO detection. To reduce the searching complexity, they build a MIMO trellis graph and split the searching operations among different nodes, where each node applyed the *M*-algorithm. Instead of keeping a global candidate list as the traditional detector does, this algorithm kept multiple small candidate lists to generate soft information. Since the DM algorithm could achieve good BER performance with a small *M*, the sorting cost of the DM algorithm was lower than that of the conventional *K*-best MIMO algorithm. The proposed algorithm was very suitable for high speed parallel processing.

Authors considered 4×4 16-QAM and 64-QAM MIMO systems where the channel matrices were assumed to have independent random Gaussian distributions. A sorted QR decomposition of the channel matrix was used. The soft-output of the detector was fed to a length 2304, rate 1/2 WiMax layered LDPC decoder, which performed up to 15 LDPC iterations and compared the BER performance with different *M* values. As a comparison, they also ploted the BER curves for the soft MAP detector with exhaustive-search and the soft linear MMSE detector. When $M = 1$, the DM detector showed about 1 dB performance loss compared to the optimal case at BER level of 10^{-5}. When $M = 2, 3$, the DM detector showed a very small performance degradation. When $M = 4$, the DM detector showed almost no performance loss. The simulation result indicated that the DM detector even with a small *M* can achieve near-ML detection performance.

Compared to the traditional *K*-best algorithm which needed to perform large sorting tasks, the proposed DM algorithm had a much lower sorting complexity which could lead to efficient high-speed hardware implementations.

Huang Chung-Jung *et. al* (2011) proposed a novel decoder for underdetermined MIMO systems with low decoding complexity. The development of the proposed decoder consisted of two stages. First, an improved slab decoding algorithm efficiently obtained

all valid candidate points within a given slab. Next, a multi-slab based decoding algorithm finds the optimal solution by conducting intersections on the obtained candidate set with dynamic radius adaptation. The proposed decoder offered the advantages of low computational complexity and near-ML decoding performance for underdetermined MIMO systems. Simulation results indicated that it effectively reduces the complexity as compared to existing decoders, especially for large antenna numbers and/or constellations.

Wu Michael *et. al* (2011) proposed a novel scalable Multiple- Input Multiple-Output (MIMO) detector that does not require preprocessing to achieve good bit error rate (BER) performance. Existing detectors such as Flexsphere used preprocessing before MIMO detection to improve performance. Instead of costly preprocessing, the proposed detector scheduled multiple search passes, where each search pass detects the transmit stream with a different permuted detection order. By changing the number of parallel search passes, they showed that their scalable detector can achieve comparable performance to Flexsphere with reduced resource requirement, or can eliminate LLR clipping and achieve BER performance within 0.25 dB of exhaustive search with increased resource requirement.

Algorithm: Proposed MIMO Detection Algorithm

1) Initialization: L←Ø

2) for i = 0 to N-1 do

3) $y_i \leftarrow$ circular rotate rows of y i times

4) $H_i \leftarrow$ circular rotate columns of H i times

5) $(y_i; R_i) \leftarrow$ MRVD-QRD($y_i; H_i$)

6) $L_i \leftarrow$ search(^yi;Ri)

7) $L_i \leftarrow L \cup L_i$

8) end

9) Compute LLR values using candidate list L

Shah Mohammad Ali *et. al* (2011) presented a novel method for the complexity reduction of MIMO detection algorithms. This method was based on the pruning of tree nodes and

the corresponding subtrees. The pruning was decided based on the absolute value of a priori information of bits greater than or equal to a threshold value. Simulation results for the TS algorithm showed that up to 25% reduction in complexity can be achieved without any BER performance degradation.

Mao Xinyu *et. al* (2011) proposed a reduced K-best sphere decoding (K-best SD) algorithm for Multiple-Input Multiple-Output (MIMO) detection. The algorithm reduced the complexity of the K-best SD by combining the statistics character of the signal and the requirement of the quality of service (QoS). In the reducing processing of the proposed algorithm, the chi-square distribution (CSD) property of the signal, the optimal symbol error rate (SER) property and the loss of pruning were considered together to give a theoretic error bound and then a threshold to determined which route can be pruned to reduced the calculation complexity. The algorithm reduced the complexity with a controllable cost of performance decrease. Simulation results on a 16-QAM system with 4×4 antennas showed that the algorithm can attain the near-optimal performance with a significant complexity reduction compared to the original K-best SD or maximum likelihood (ML) algorithm.

Li Guanghui *et. al* (2012) proposed fixed-complexity sphere decoder (FSD) to attain the near-optimal performance achieving the same diversity order as the maximum-likelihood decoder (MLD) recently. However, it suffered great redundant computations resulting in high power consumption. So in this paper, they conducted an improved algorithm for the original FSD by using early termination (ET). Their algorithm preserved the advantages of sphere decoder (SD) such as branch pruning and an adaptively updated pruning threshold. They compared the proposed algorithm with the original FSD and a lately developed statistical threshold-based FSD (ST-FSD). Simulation results demonstrated that the proposed algorithm attains the same performance with a much lower cost than the FSD.

Li. Shi-Ping *et. al*. (2012) To solve the problem of calculation complexity, authors used the sorting algorithm in sphere decoding algorithm. To apply the sorting algorithm which comes from sorted QR decomposition algorithm to the sphere decoding algorithm, they

used the ordered sphere decoding detection algorithm. With the simulation results, they showed that the novel algorithm not only keep the same performance as the traditional sphere decoding algorithm, but also efficiently decreases the calculation complexity of the sphere decoding algorithm.

Wu Michael *et. al* (2012) proposed a flexible Multiple-Input Multiple-Output (MIMO) detector. Existing detectors either used costly sorting for better performance or sacrificed sorting for higher throughput. To achieve good performance with high throughput, authors' detector runs multiple search passes in parallel, where each search pass detected the transmit stream with a different permuted detection order. They showed that their flexible detector, including QR decomposition preprocessing, outperforms existing MIMO detectors while maintaining good bit error rate (BER) performance. In addition, their detector achieved different tradeoffs between throughput and accuracy by changing the number of parallel search passes.

Wu Michael *et. al* (2012) presented a novel low complexity scalable multiple-input multiple-output (MIMO) detector that does not require preprocessing and the optimal squared l2-norm computations to achieve good bit error (BER) performance. Unlike existing detectors such as Flexsphere that used preprocessing before MIMO detection to improve performance, the proposed detector instead performed multiple search passes, where each search pass detects the transmit stream with a different permuted detection order. In addition, to reduce the number of multipliers required in the design, they used l1-norm in place of the optimal squared l2-norm. To ameliorate the BER performance loss due to l1- norm, they also proposed squaring then scaling the l1-norm. By changing the number of parallel search passes and using norm scaling, they showed that their design achieved comparable performance to Flexsphere with reduced resource requirement or achieves BER performance close to exhaustive search with increased resource requirement.

Radosavljevic Predrag *et. al* (2012) described implementation of a detector with parallel partial candidate-search algorithm. Two fully independent partial candidate search processes were simultaneously employed for two groups of transmit antennas based on

QR decomposition (QRD) and QL decomposition (QLD) of a multiple-input multiple-output (MIMO) channel matrix. By using separate simultaneous candidate searching processes, the proposed implementation of QRD-QLD searching-based sphere detector provided a smaller latency and a lower computational complexity than the original QRD-M detector for similar error-rate performance in wireless communications systems employing four transmit and four receive antennas with 16-QAM or 64-QAM constellation size.

The QRD-QLD-PD was compared in terms of computational complexity, detection latency and error-rate performance with the QRD-M detector proposed for several emerging wireless technologies. It is shown in this work that a search latency of the QRD-QLD-PD is smaller than that of the QRD-M detector for same error-rate performance. Further, implementation complexity (i.e., a number of arithmetic operations) associated with the QRD-QLD-PD was shown to be substantially smaller than that of the QRD-M detector for the same error rate performance.

The FPGA and ASIC synthesis results for the QRD-QLD-PD also showed smaller design complexity than that of the QRD-M detector. Finally, ASIC design results of the QRD-QLD-PD were compared with that of other sphere decoders reported in the literature and showed that the QRD-QLD-PD has comparatively advantages over related solutions from the literature, or comparable design results.

Han Shuangshuang *et. al* (2012) The conventional K-best sphere decoder (KSD) keeps the best K nodes at each level of the search tree, so in addition to retaining the best K nodes, authors also considered all the nodes whose costs were within a certain margin of the cost of the Kth best node. The resulting algorithm was called improved K-best sphere decoder (IKSD). Three IKSD variants were considered, which were fixed threshold, normalized threshold and adaptive threshold IKSD. The proposed IKSD required a smaller K (indicating lower complexity) while still achieving a better and near optimal performance compared to the conventional KSD. These gains are confirmed by the simulation results.

Sun Yang *et. al* (2012) proposed a novel path-preserving trellis-search (PPTS) algorithm and its high-speed VLSI architecture for soft-output multiple-input-multiple-output (MIMO) detection. They represented the search space of the MIMO signal with an unconstrained trellis, where each node in stage k of the trellis maps to a possible complex-valued symbol transmitted by antenna. Based on the trellis model, they converted the soft-output MIMO detection problem into a multiple shortest paths problem subject to the constraint that every trellis node must be covered in this set of paths. The proposed detector was guaranteed to have soft information for every possible symbol transmitted on every antenna so that the log-likelihood ratio (LLR) for each transmitted data bit can be more accurately formed. Simulation results showed that the proposed algorithm achieved near-optimal error performance with a low search complexity and also was hardware-friendly.

The proposed systolic PPTS detector can achieve a 6.4 Gbps throughput when running at 400 MHz. The proposed detectors achieved very high data throughput while still maintaining a low area requirement. Compared to the K-Best detector, the PPTS detectors have a better area efficiency. The PPTS detector achieved a balanced tradeoff between hardware complexity and error performance. The PPTS detector also achieved a close-to-optimal error performance with a reasonable hardware cost. Therefore, the proposed detector is a viable solution for the Gbps MIMO detection problem as it achieves both high throughput performance and good error performance.

Sun Yang *et. al* (2012) proposed a trellis-search based soft-input soft-output detection algorithm and its VLSI architecture for iterative multiple-input multiple- output (MIMO) receivers. They constructed a trellis diagram to represent the search space of a transmitted MIMO signal. With the trellis model, they evenly distributed the workload of candidates searching among multiple trellis nodes for parallel processing. The search complexity was significantly reduced because the number of candidates were greatly limited at each trellis node. By leveraging the trellis structure, they also developed an approximate Log-MAP algorithm by using a small list of largest exponential terms to compute the LLR (log-likelihood ratio) values. The trellis-search based detector had a fixed-complexity and was very suitable for parallel VLSI implementation.

CHAPTER 3
QR DECOMPOSITION

3.1 QR Decomposition

Theorem: Any $\mathbf{A}\epsilon\mathbb{R}^{nxm}$ (n ≥ m) has a QR decomposition:

$$\mathbf{A}=Q\ R$$

Where Q is n x n orthogonal matrix and R *is* upper triangular matrix. The same theorem can be proven constructively via the two special classes of orthogonal matrices i.e. rotation and reflection (Myllylä M., 2005).. The same decomposition can also be implemented using Gram Schmitt orthogonalization, Household transformation, Givens rotation and sorted QR decomposition.

In the presented work, we have modified the sphere decoding algorithm by changing the way in which we are getting the QR decomposition. We have applied all the above four specified decomposition techniques to obtain Q and R.

3.2 QR Decomposition by Gram Schmitt Orthogonalization

Another method for computing the QR factorization is the Gram-Schmidt orthogonalization process. Given two vectors a_1 and a_2, we can determine two orthonormal vectors q_1 and q_2 that span the same subspace by orthogonalizing one of the given vectors against the other, as shown in Figure 3.1 (Heath M. T., 1997).

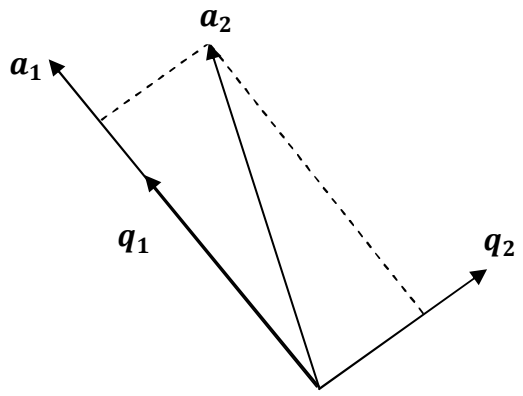

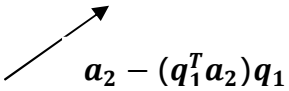

Figure 3.1: One step of Gram-Schmidt orthogonalization.

This process can be extended to an arbitrary number of vectors a_k (up to the dimensionof the space) by orthogonalizing each successive vector against all of the previous ones, giving the classical Gram-Schmidt orthogonalization.

If we take the a_k to be the columns of the matrix **A**, then the resulting q_k are the columns of Q and the r_{ij} are the entries of the upper triangular matrix R in the QR factorization of **A**. Unfortunately, the classical Gram-Schmidt procedure requires separate storage for **A**, Q, and R because the original a_k are needed in the inner loop, and hence the q_k cannot overwrite the columns of **A** (Heath M. T., 1997).. This shortcoming can be alleviated, however, if we orthogonalize each chosen vector in turn against all of the subsequent vectors, in effect generating the upper triangular matrix R by rows rather than by columns. This rearrangement of the computation is known as modified Gram-Schmidt orthogonalization.

Now a_k and q_k share the same storage. Unfortunately, separate storage for Q and R is still required, a disadvantage compared with the Householder method, for which Q and R can share the space formerly occupied by **A** (Heath M. T., 1997). On the other hand, Gram-Schmidt provides an explicit representation for Q, which, if desired, would require additional storage with the Householder method.

In addition to requiring less storage than the classical procedure, an added bonus of modified Gram-Schmidt is that it is also numerically superior to classical Gram-Schmidt: the two procedures are mathematically equivalent, but the classical procedure tends to lose orthogonality among the computed q_k. Although the modified Gram-Schmidt procedure has advantages in some circumstances, for solving least squares problems it is somewhat inferior to the Householder method in storage, work, and accuracy.

3.3 QR Decomposition by Household Transformation

Given vectors $x \neq y$ satisfying $\|x\|_2 = \|y\|_2$, there is a Household transformation **P** such that **P**.$x = y$.

where $\mathbf{P} = I - 2uu^T$, and $u = (x - y)/\|x - y\|_2$

P.x is the reflection of x in the plane through the origin and perpendicular to u as shown in figure 3.2 (Heath M. T., 1997).

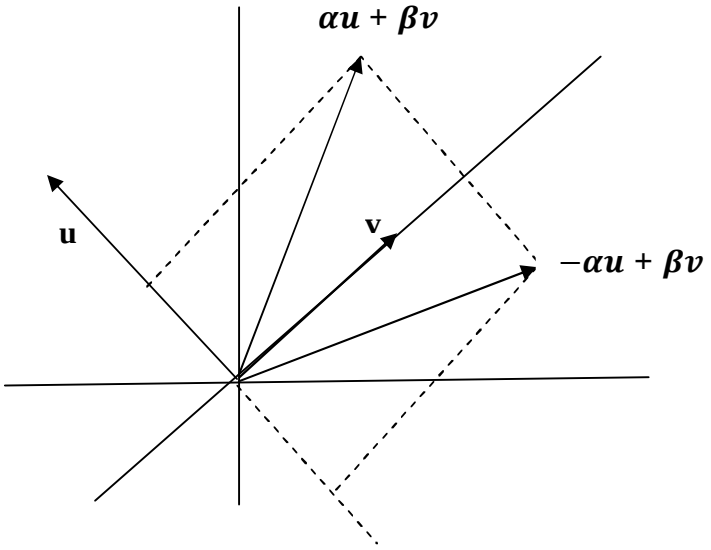

Figure 3.2: Reflection of a vector.

Household transformation **P** has the properties of symmetry and orthogonality.

Household transformation **P** can be used to transform any vector x into a multiplier of e_1 as (Heath M. T., 1997) **P**.x $\equiv (I - 2uu^T)x = \alpha e_1$.

First the Household transformation can transform **P** = $(I - 2uu^T)$, which can be used to transform a vector x into a multiplier of e_1. **P**.x $\equiv (I - 2uu^T)x = \alpha e_1$: **P**.x= $\mathbf{P}\begin{pmatrix}\alpha\\0\\\vdots\\0\end{pmatrix}$

If we extend the vector x to the matrix $\mathbf{A} \in \mathbb{R}^{nxm}$, then finds $P_1 = I - 2uu^T$ that transforms $\mathbf{A}e_1$ into a multiplier of e_1:

$$P_1A = \left[\begin{array}{c|c} x & x \cdots x \\ \hline 0 & x \cdots x \\ \vdots & \vdots \\ 0 & x \cdots x \end{array}\right]$$

And then the process proceeds to work on the side corner submatrix in exactly the same way.

In applying Household transformation P to arbitary vector x, $Px = (I - 2\frac{vv^T}{v^Tv})$x = x – $(2\frac{vv^T}{v^Tv})v$ which is subtantially cheaper to compute than general matrix-vector multiplication (Trefethen and Bau.,1997).

- The factorization requires about $2m^2(n - m/3)$ FLOPs (multiplications plus additions)
- With m = n we require about $4m^3/3$ FLOPs
- Gaussian elimination requires about $2m^3/3$ FLOPs

3.4 QR Decomposition by Givens rotation

On a 2-diamentional plane if we have to find a 2 x 2 matrix Q, so that Q.*x* equals a rotated vector *x* through a fixed angle θ, then to determine Q, we just need to examine the unit basis vector e_1 and e_2, as shown in figure 3.3 (Heath M. T., 1997).

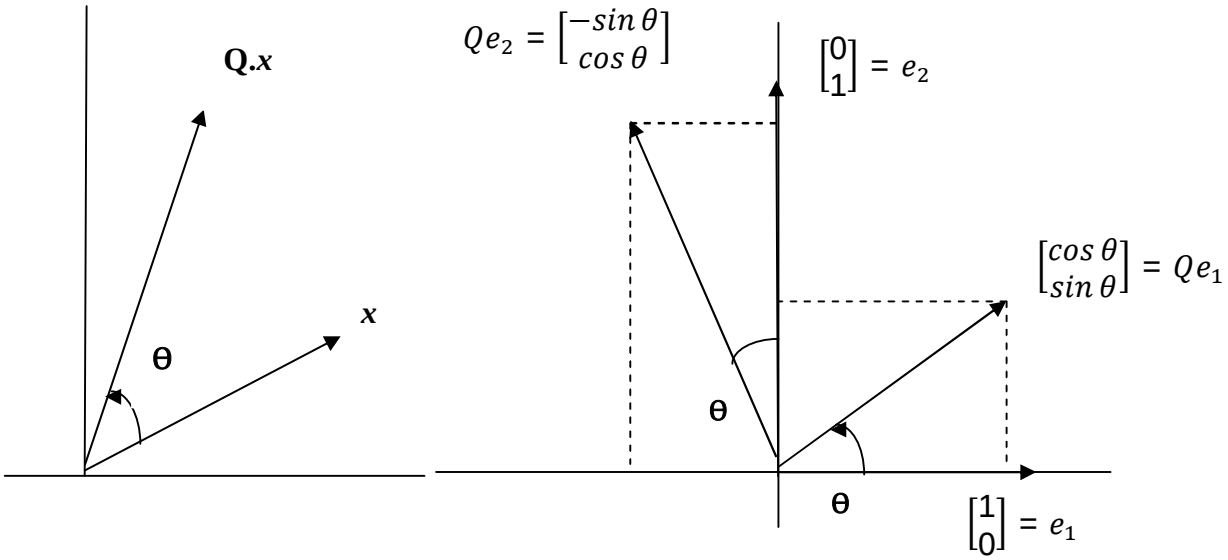

Figure 3.3: Rotation of a vector x by an angle θ.

From the figure, Q = $\begin{pmatrix} cos\theta & sin\theta \\ -sin\theta & cos\theta \end{pmatrix} = \begin{pmatrix} c & s \\ -s & c \end{pmatrix}$

Now any vector *x* = $\begin{pmatrix} x_1 \\ x_2 \end{pmatrix}$ can be rotated to the unit vector e_1 direction as:

$$\begin{pmatrix} c & s \\ -s & c \end{pmatrix}^T \begin{pmatrix} x_1 \\ x_2 \end{pmatrix} = \begin{pmatrix} r \\ 0 \end{pmatrix}$$

where $c = \frac{x_1}{\sqrt{(x_1{}^2+x_2{}^2)}}$ and $s = \frac{x_2}{\sqrt{(x_1{}^2+x_2{}^2)}}$,

we have $Q^T x = re_1$, where $r = \sqrt{(x_1{}^2 + x_2{}^2)} = \|x\|_2$.

It essentially works on the $i^{th} - j^{th}$ plane only (Heath M. T., 1997).

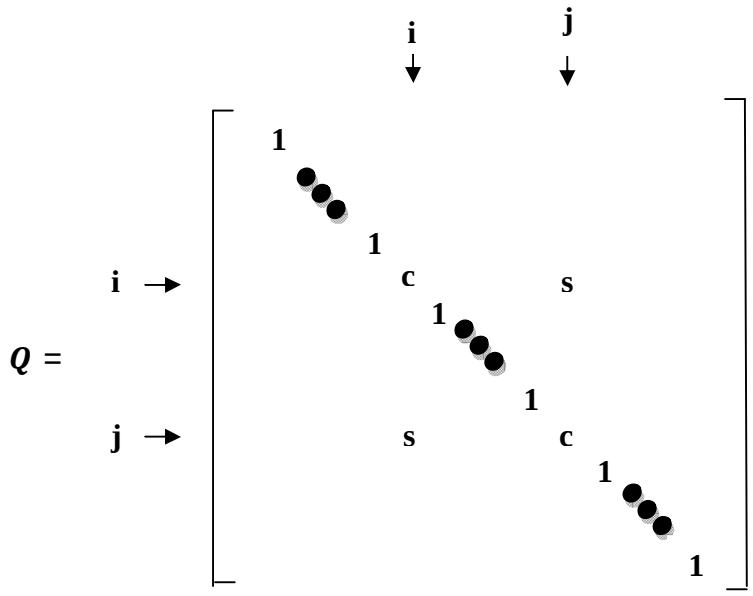

In general, the algorithm works on one component at a time. The first column needs n-1 rotators which transform $\mathbf{A} \epsilon \mathbb{R}^{nxm}$ into

$$Q_{n1}^T Q_{n-11}^T \cdots Q_{31}^T Q_{21}^T A = \begin{bmatrix} x & x \cdots x \\ 0 & x \cdots x \\ \vdots & \vdots \\ 0 & x \cdots x \end{bmatrix}$$

The process proceeds to work on the right corner submatrix in exactly the same way.

- The factorization requires about $3m^2(n - m/3)$ multiplications and additions
- Reflections require $2m^2(n - m/3)$ FLOPs
- Reflections are generally preferred

3.5 QR Decomposition by Sorted QR decomposition

QR factorization of **H** is performed as:

$$\mathbf{H = QR}$$

where Q is N_R x N_T unitary matrix and R is an N_R x N_T upper triangular matrix. Multiplying by Q^H on both the sides of equality in the equation **y = H.x + n**, and expanding it, we get (Myllylä M., 2011)

$$\begin{pmatrix} y_1' \\ y_2' \\ \vdots \\ y_{N_T}' \end{pmatrix} = \begin{pmatrix} r_{1,1} & r_{1,2} & \cdots & r_{1,N_T} \\ 0 & r_{2,2} & \cdots & r_{2,N_T} \\ \vdots & \vdots & \ddots & \vdots \\ 0 & 0 & \cdots & r_{N_T,N_T} \end{pmatrix} \begin{pmatrix} x_1 \\ x_2 \\ \vdots \\ x_{N_T} \end{pmatrix} + \begin{pmatrix} n_1' \\ n_2' \\ \vdots \\ n_{N_T}' \end{pmatrix}$$

If we calculate this equation from the bottom to the top, we can get the x_{N_T} from $y_T^{'} = r_{N_T,N_T}x_{N_T} + n_{N_T}$ at first, and according to quantization and decision, we can obtain the estimated signal $\overline{x_{N_T}}$ of the last antenna. Then insert $\overline{x_{N_T}}$ into the second line from the bottom and we can acquire the signal $\overline{x_{N_T-1}}$. Continuing this calculation and at last we will obtain all the signals of multiple antennas. This process is the principle of QR algorithm. However, if there are some errors in the signal detection of the (k)th row caused by signal error propagation, all the signals above the (k)th row would be effected by the signal of the (k)th row. In order to avoid this thing to happen and to minimize the bit error rate (BER) of detection, algorithm should detect the signal of the minimum estimated error in each step at first (LI Shi-Ping., 2012). So, the best sorted matrix R should maximize the, $|r_{k,k}|$ in every step of detection to maximize the signal-to-noise ratio (SNR).

SQRD algorithm is based on the theory of modified Gram-Schmidt orthogonalization methods. It combines the process of searching the detection sequence with the QR factorization and sorts the columns of channel matrix before orthogonalization every time. SQRD algorithm differs from QR algorithm in that the column of H is permuted, i.e.

$$\overline{\boldsymbol{Q}}\,\overline{\boldsymbol{R}} = \mathbf{HP}$$

where **P** is a permute matrix and $\boldsymbol{P^H P = I}$. **P**'s function is to maximize the SNR in the (k)th (k= $N_T, N_T - 1, \ldots, 1$) step. But it's too complicated to find the best **P**, so the

SQRD algorithm based on the strategy that to make the upper of R have the less SNR to find **P**, so that the diagonal elements $|r_{k,k}|$ of the left upper part of R would have less value (LI Shi-Ping., 2012). In the process of permuting the columns of **Q**, SQRD algorithm prior compute the column which orthogonal by $q_i, q_{i-1}, \cdots, q_{N_T}$ and $q_1, q_2, \cdots, q_{i-1}$ of **Q** and own the minimum-norm, after that, the diagonal elements' value of **R** are ranged from little to large, and the best permute matrix P is found out.

On applying the sorting method of SQRD algorithm into the QR factorization of SD algorithm, to make sure that the signals of each layer are ordered with the SNR from high to low, so that the SD algorithm can prior detect the signal which own the maximum SNR, and because of this measure, SD algorithm doesn't need to detect the signals with low SNR (LI Shi-Ping., 2012) and this helps to decrease the possibility of algorithm searching paths be cut off so that the calculation complexity can be decreased. The Sorted QR Decomposition decreases the number of visited nodes approximately 20% on average compared to the conventional QR decomposition (Myllylä M., 2011).

3.6 A comparison of decomposition Methods

A straightforward implementation of Givens method requires more work than Householder method. Because Givens works on one component at a time but, Householder works on one column at a time, and Givens also requires more storage, since each rotation requires two numbers, c and s to define it. Also it has been found that almost 4% floating point operations per second (FLOPS) are saved if we use make use of sorted QR decomposition to obtain Q and R matrix (LI Shi-Ping., 2012). But we can't say that Householder is better than Givens or Sorted QR as that depends on situation.

For solving dense linear least squares problems, the Householder method is generally the most efficient and accurate of the orthogonalization methods. It requires about $n^2m - n^3/3$ multiplications and a similar number of additions. The Householder method produces a solution whose relative error is proportional to cond(**A**)+$\|r\|_2[cond(\boldsymbol{A})]^2$, (Trefethen and Bau.,1997) which is the best that can be expected since this is the inherent sensitivity of the solution to the least squares problem itself.

The condition number cond(.) is a measure of how close a matrix is to being singular: a matrix with a large condition number is nearly singular, whereas a matrix with a condition number close to 1 is far from being singular (Heath M. T., 1997). Moreover, the Householder method can be expected to break down (in the back-substitution phase) only if cond(A) is worst.

For nearly square problems, $m \approx n$, the normal equations and Householder methods require about the same amount of work. But for highly overdetermined problems, $m \gg n$, the Householder method requires about twice as much work as the normal equations method. On the other hand, the Householder method is more accurate and more broadly applicable than the normal equations method. These advantages may not be worth the additional cost, however, when the problem is sufficiently well-conditioned that the normal equations method provides adequate accuracy. The SQRD preprocessing, however, decreases the number of visited nodes approximately 20% on average compared to the QRD (Myllylä M., 2011).

CHAPTER 4
MIMO SIGNAL DETECTION

4.1 Signal Detection for Spatially Multiplexed MIMO Systems

High speed data transmission can be achieved through spatially multiplexed MIMO (SM-MIMO) systems. However, spatial demultiplexing at the receiver side is a challenging task for SM MIMO systems. Consider the $\mathbf{N_R}$x $\mathbf{N_T}$ MIMO system in Figure 4.1. Let **H** denote a channel matrix with it $(j.i)^{th}$ entry$\mathbf{h_{ji}}$ for the channel gain between the i^{th} transmit antenna and the j^{th} receive antenna, j=1, 2, ... ,$\mathbf{N_R}$ and i= 1, 2, ... ,$\mathbf{N_T}$. The spatially-multiplexed user data and the corresponding received signals are represented by $\mathbf{x}=[x1, x2, \ldots, x_{N_T}]^T$ and $\mathbf{y}=[y1, y2, \ldots, y_{N_R}]^T$ respectively (Cho S. Y., 2012), where x_i and y_j denote the transmit signal from the i^{th} transmit antenna andthe received signal at the j^{th} receive antenna, respectively. Let z_j denote the white Gaussiannoise with a variance of σ_z^2at the j^{th} receive antenna, and h_i denote the i^{th} column vector ofthe channel matrix H. Now, the $\mathbf{N_R}$x $\mathbf{N_T}$ MIMO system is represented as (Myllylä M., 2009).

$$\mathbf{y = Hx + z}$$
$$\mathbf{= h_1x_1 + h_2x_2 + \ldots + h_{N_T}x_{N_T} + z} \qquad (4.1)$$

where $\mathbf{z} = [z1, z2, \ldots, z_{N_R}]^T$.

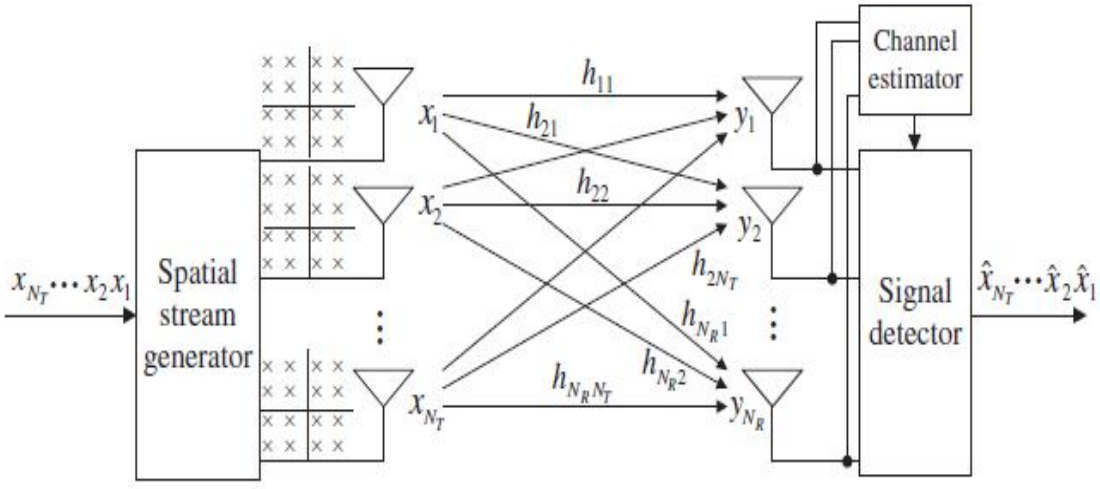

Figure 4.1: Spatially multiplexed MIMO systems (Cho S. Y., 2012).

4.2 Linear Signal Detection

Linear signal detection method treats all transmitted signals as interferences except for the desired stream from the target transmit antenna. Therefore, interference signals from other transmit antennas are minimized or nullified in the course of detecting the desired signal from the target transmit antenna (Bai L., 2012). To facilitate the detection of desired signals from each antenna, the effect of the channel is inverted by a weight matrix W such that (Cho S. Y., 2012)

$$\tilde{\mathbf{x}} = [\widetilde{x_1}\,\widetilde{x_2} \ldots \widetilde{x_{N_T}}]^T = \mathbf{W}\mathbf{y} \tag{4.2}$$

that is, detection of each symbol is given by a linear combination of the received signals. The standard linear detection methods include the zero-forcing (ZF) technique and the minimum mean square error (MMSE) technique.

4.2.1 ZF Signal Detection

The zero-forcing (ZF) technique nullifies the interference by the following weight matrix:

$$\mathbf{W}_{ZF} = (\mathbf{H}^{\mathbf{H}}\mathbf{H})^{-1}\mathbf{H}^{\mathbf{H}} \tag{4.3}$$

where $(.)^H$ denotes the Hermitian transpose operation. In other words, it inverts the effect of channel as (Cho S. Y., 2012)

$$\begin{aligned}\widetilde{\mathbf{x}_{\mathbf{ZF}}} &= \mathbf{W}_{\mathbf{ZF}}\mathbf{y} \\ &= \mathbf{x} + \widetilde{\mathbf{z}_{\mathbf{ZF}}}\end{aligned} \tag{4.4}$$

where $\widetilde{\mathbf{z}_{\mathbf{ZF}}} = \mathbf{W}_{\mathbf{ZF}}\mathbf{z} = (\mathbf{H}^{\mathbf{H}}\mathbf{H})^{-1}\mathbf{H}^{\mathbf{H}}\mathbf{z}$. Thus the error performance is directly related to the power of $\widetilde{\mathbf{z}_{\mathbf{ZF}}}$ (i.e.$\|\widetilde{\mathbf{z}_{\mathbf{ZF}}}\|_2^2$).

The expected value of the noise power is given as (Cho S. Y. 2012)

$$\mathrm{E}\{\|\widetilde{\mathbf{z}_{\mathbf{ZF}}}\|_2^2\} = \sum_{i=1}^{N_T} \frac{\sigma_z^2}{\sigma_i^2} \tag{4.5}$$

4.2.2 MMSE Signal Detection

In order to maximize the post-detection signal-to-interference-plus-noise ratio (SINR), the MMSE weight matrix is given as (Cho S. Y. 2012)

$$\mathbf{W}_{\mathbf{MMSE}} = (\mathbf{H}^{\mathbf{H}}\mathbf{H} + \boldsymbol{\sigma}_{\mathbf{z}}^{\mathbf{2}}\mathbf{I})^{-1}\mathbf{H}^{\mathbf{H}} \tag{4.6}$$

MMSE receiver requires the statistical information of noise$\boldsymbol{\sigma}_{\mathbf{z}}^{\mathbf{2}}$.Using the MMSE weight in Equation (4.6), we obtain the following relationship: (Cho S. Y. 2012)

$$\widetilde{\mathbf{x}_{\mathbf{MMSE}}} = \mathbf{W}_{\mathbf{MMSE}}\mathbf{y}$$

$$= \tilde{\mathbf{x}} + \widetilde{\mathbf{z}_{\mathbf{MMSE}}} \quad (4.7)$$

The expected value of $\widetilde{\mathbf{z}_{\mathbf{MMSE}}}$ is given as (Cho S. Y. 2012)

$$\mathrm{E}\{\|\widetilde{\mathbf{z}_{\mathbf{MMSE}}}\|_2^2\} = \sum_{i=1}^{N_T} \frac{\boldsymbol{\sigma_z^2 \sigma_i^2}}{(\boldsymbol{\sigma_z^2 + \sigma_i^2})^2} \quad (4.8)$$

Noise enhancement effect in the course of linear filtering is significant when the condition number of the channel matrix is large, that is, the minimum singular value is very small. Comparing Equation (4.5) to Equation (4.8), it is clear that the effect of noise enhancement in MMSE filtering is less critical than that in ZF filtering. If $\sigma_{\min}^2 \gg \sigma_z^2$ and thus $\sigma_{\min}^2 + \sigma_z^2 \approx \sigma_{\min}^2$, then the noise enhancement effect of the two linear filters becomes the same (Cho S. Y. 2012). The diversity order achieved by the ZF technique is $N_R - N_T + 1$. In thecase of the single transmit antenna and multiple receive antennas, a ZF receiver is equivalent to amaximal ratio combining (MRC) receiver that achieves the diversity order of N_R.

4.3 OSIC Signal Detection

In general, the performance of the linear detection methods is worse than that of other nonlinear receiver techniques. However, linear detection methods require a low complexity of hardware implementation. We can improve their performance without increasing the complexity significantly by an ordered successive interference cancellation (OSIC) method (Bai L., 2012). It is a bank of linear receivers, each of which detects one of the parallel data streams, with the detected signal components successively canceled from the received signal at each stage. More specifically, the detected signal in each stage is subtracted from the received signal so that the remaining signal with the reduced interference can be used in the subsequent stage.

Figure 4.2 illustrates the OSIC signal detection process for four spatial streams. Let $x_{(i)}$denote the symbol to be detected in the i^{th} order, which may be different from the transmitsignal at the i^{th} antenna, since $x_{(i)}$depends on the order of detection. Let $\widehat{x_{(i)}}$ denote a slicedvalue of $x_{(i)}$. In the course of OSIC, either ZF method in Equation (4.3) or MMSE method in Equation (4.6) can be used for symbol estimation.

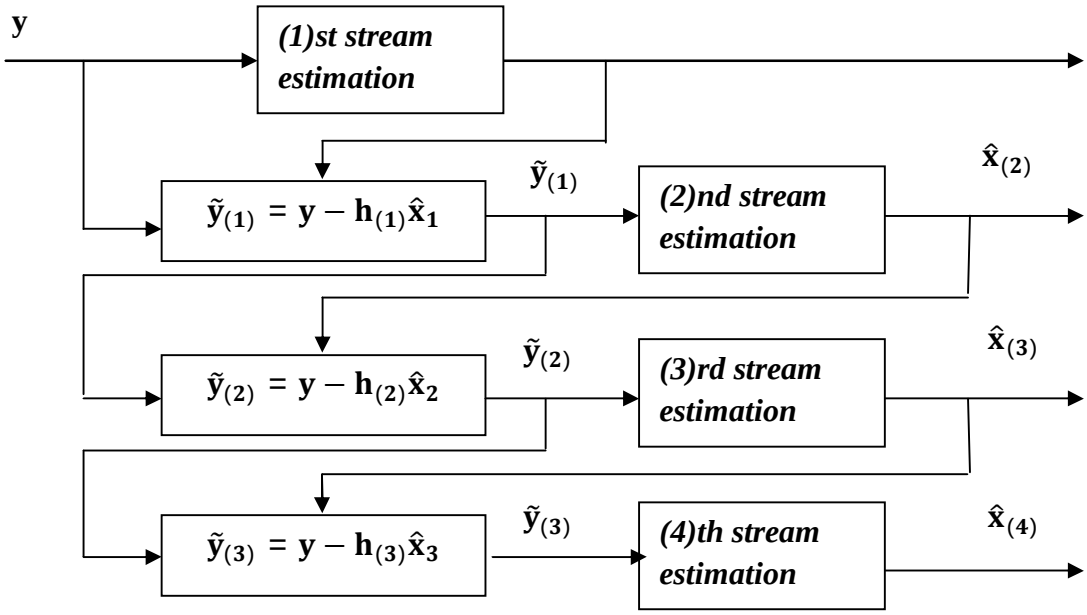

Figure 4.2 Illustration of OSIC signal detection for four spatial streams (i.e.N_T = 4). (Cho S. Y., 2012)

The (1)st stream is estimated with the (1)st row vector of the MMSE weight matrix in Equation (4.6). After estimation and slicing to produce $\widetilde{x_{(1)}}$, the remaining signal in the first stage is formed by subtracting it from the received signal, that is, (Cho S. Y., 2012)

$$\tilde{\mathbf{y}}_{\mathbf{1}} = \mathbf{y} - \mathbf{h}_{(1)}\tilde{\mathbf{x}}_{(1)}$$
$$= \mathbf{h}_{(1)}\left(\mathbf{x}_{(1)} - \tilde{\mathbf{x}}_{(1)}\right) + \mathbf{h}_{(2)}\mathbf{x}_{(2)} + \mathbf{h}_{(\mathbf{N_T})}\mathbf{x}_{\mathbf{N_T}} + \mathbf{z} \quad (4.9)$$

If $\mathbf{x}_{(1)} = \tilde{\mathbf{x}}_{(1)}$, then the interference is successfully canceled in the course of estimating $x_{(2)}$; however, if $\mathbf{x}_{(1)} \neq \tilde{\mathbf{x}}_{(1)}$, then error propagation is incurred because the MMSE weight that hasbeen designed under the condition of $\mathbf{x}_{(1)} = \tilde{\mathbf{x}}_{(1)}$is used for estimating $x_{(2)}$.Due to the error propagation caused by erroneous decision in the previous stages, the order of detection has significant influence on the overall performance of OSIC detection. Using the OSIC method, the diversity order can be larger than $N_R - N_T + 1$ for all symbols. Thanks to ordering, the diversity order of the first-detected symbol is also larger than$N_R - N_T + 1$ (Bai L., 2012). However, the rest of symbols have the diversity order that depends on whether the previously-detected symbols are correct or not. If they are all correct, the diversity order of the i^{th}detected symbol becomes $N_R - N_T + i$.

4.4 ML Signal Detection

Maximum likelihood (ML) detection calculates the Euclidean distance between the received signal vector and the product of all possible transmitted signal vectors with the given channel **H**, and finds the one with the minimum distance (Damen M. O., 2003). Let C and N_T denote a set of signal constellationsymbol points and a number of transmit antennas, respectively. Then, ML detection determines the estimate of the transmitted signal vector **x** as (Bai L., 2012)

$$\hat{\mathbf{x}}_{\mathrm{ML}} = \arg \min_{s \epsilon C^{N_T}} \|\mathbf{y} - \mathbf{H}\mathbf{x}\|^2 \tag{4.10}$$

where $\|\mathbf{y} - \mathbf{H}\mathbf{x}\|^2$corresponds to the ML metric. The ML method achieves the optimalperformance as the maximum a posteriori (MAP) detection when all the transmitted vectorsare equally likely. However, its complexity increases exponentially as modulation order and/or the number of transmit antennas increases. The required number of ML metric calculation is $|C|^{N_T}$, that is, the complexity of metric calculation exponentially increases with the number of antennas (Hassibi B., 2005).

The $N_T C$ values are described in Table 1. Table 2 shows the exhaustive searching number of ML. When using four transmit antennas and 64-QAM modulation, the number of searching calculation is 16 million! It is very difficult to search so many points to reach to the optimal solution.

Table 1: $N_T C$ value with respect to antenna number and modulation scheme.

$2T_R$ + 16-QAM	8
$2T_R$ + 32-QAM	10
$2T_R$ + 64-QAM	12
$3T_R$ + 16-QAM	12
$3T_R$ + 32-QAM	15
$3T_R$ + 64-QAM	18
$4T_R$ + 16-QAM	16
$4T_R$ + 32-QAM	20
$4T_R$ + 64-QAM	24

Table 2: Number of search calculation for ML detector.

Mode	Number of nodes
$2T_R$ + 16-QAM	2^{2x4} = 256
$2T_R$ + 32-QAM	2^{2x5} =1024
$2T_R$ + 64-QAM	2^{2x6} =4,096
$3T_R$ + 16-QAM	2^{3x4} = 4,096
$3T_R$ + 32-QAM	2^{3x5} = 32,768
$3T_R$ + 64-QAM	2^{3x6} = 2,62,144
$4T_R$ + 16-QAM	2^{4x4} = 65,536
$4T_R$ + 32-QAM	2^{4x5} = 10,48,576
$4T_R$ + 64-QAM	2^{4x6} = 16,777,216

Even if this particular method suffers from computational complexity, its performance serves as a reference to other detection methods since it corresponds to the best possible performance. It has been shown that the number of ML metric calculations can be reduced from $|C|^{N_T}$ to $|C|^{N_T-1}$by the modified ML (MML) detection method. In other words, it will be useful for reducing the complexity when N_T = 2. However, its complexity is still too much for $N_T \geq 3$ (Hassibi B., 2005).

The linear detection methods and OSIC detection methods require much lower complexity than the optimal ML detection, but their performance is significantly inferior to the ML detection. It is obvious that the ML detection outperforms the OSIC detection (Sun Y., 2012). Therefore, there have been active researches to develop the detection methods that still consider the ML detection criterion in Equation (4.10) while still achieving a near-optimal performance with less complexity.

4.5 Sphere Decoding Method

The Nondeterministic Polynomial-time hard (NP-hard) complexity of Maximum Likelihood (ML) decoding, the optimal decoder, prohibits its use in practical Multiple-Input Multiple-Output (MIMO) systems, especially when a large signal constellation and/or many transmit antennas are involved (Sun Y., 2012). Some suboptimum detection algorithms, such as Kannan's algorithm which searches only over restricted

parallelograms, the KZ algorithm based on the Korkin-Zolotarev-reduced basis, and the Sphere Decoding (SD) algorithm of Fincke and Pohst, can perform detection with much lower complexity, but at a performance degradation (Cho S. Y., 2012).

SD was first introduced to perform ML detection, and it achieves reduced complexity by searching for the closest lattice point over the points that lie in a certain sphere around a given vector. Although it significantly reduces the computational complexity of ML, it requires huge amount of computations in MIMO systems. There are several approaches to reduce the complexity of SD algorithm such as the Schnorr-Euchner (SE) enumeration, descending probabilistic ordering, increasing radius sphere decoder, parallel competing branch algorithm, and reduced dimension maximum likelihood search (Hassibi B., 2005). Various researchers have analyzed the complexity of SD which shows that the expected complexity of SD i.e. the expected number of operations required by the algorithm, depends on the both number of transmit antennas N_T, and the Signal-to-Noise Ratio (SNR), ρ. Also with high SNR, the expected number of operations required by the SD, can be approximated by a polynomial function for small N_T (Jald´en, J., 2005).

Sphere decoding (SD) method intends to find the transmitted signal vector with minimum ML metric. It considers only a small set of vectors within a given sphere rather than all possible transmitted signal vectors. SD adjusts the sphere radius until there exists a single vector (ML solution vector) within a sphere (Stojnic M., 2008). It increases the radius when there exists no vector within a sphere, and decreases the radius when there exist multiple vectors within the sphere.

Considering a square QAM in a 2x2 complex MIMO channel. The underlying complex system can be converted into an equivalent real system. Let y_{jR} and y_{jI} denote the real and imaginary parts of the received signal at the j^{th} receive antenna, that is, $y_{jR} = Re(y_j)$ and $y_{jI} = Im(y_j)$. Similarly, the input signal x_i from the i^{th} antenna can be represented in the similar manner.

$$\begin{bmatrix} y_{1R} \\ y_{2R} \\ y_{1I} \\ y_{2I} \end{bmatrix} = \begin{bmatrix} h_{11R} & h_{21R} & -h_{11I} & -h_{12I} \\ h_{21R} & h_{22R} & -h_{21I} & -h_{22I} \\ h_{11I} & h_{12I} & h_{11R} & h_{12R} \\ h_{21I} & h_{22I} & h_{21R} & h_{22R} \end{bmatrix} \begin{bmatrix} x_{1R} \\ x_{2R} \\ x_{1I} \\ x_{2I} \end{bmatrix} + \begin{bmatrix} z_{1R} \\ z_{2R} \\ z_{1I} \\ z_{2I} \end{bmatrix} \quad (4.11)$$

For $\bar{\mathbf{y}}$, $\bar{\mathbf{H}}$, $\bar{\mathbf{x}}$, and $\bar{\mathbf{z}}$ defined in Equation (4.11), the SD method exploits the following relation: (Cho S. Y., 2012)

$$\arg\min_{\bar{x}}\|\mathbf{y}-\mathbf{Hx}\|^2 = \arg\min_{\bar{\mathbf{x}}}(\bar{\mathbf{x}}-\hat{\bar{\mathbf{x}}})^{\mathbf{T}}\bar{\mathbf{H}}^{\mathbf{T}}\bar{\mathbf{H}}\,(\bar{\mathbf{x}}-\hat{\bar{\mathbf{x}}}) \tag{4.12}$$

where $\hat{\bar{\mathbf{x}}} = (\bar{\mathbf{H}}^{\mathbf{H}}\bar{\mathbf{H}})^{-1}\bar{\mathbf{H}}^{\mathbf{H}}\bar{\mathbf{y}}$, which is the unconstrained solution of the real system shown in Equation (4.11). Equation (4.12) shows that the ML solution can be determined by the different metric $(\bar{\mathbf{x}}-\hat{\bar{\mathbf{x}}})^{\mathbf{T}}\bar{\mathbf{H}}^{\mathbf{T}}\bar{\mathbf{H}}\,(\bar{\mathbf{x}}-\hat{\bar{\mathbf{x}}})$. Considering the sphere with the radius of R_{SD}: (Sun Y., 2012)

$$(\bar{\mathbf{x}}-\hat{\bar{\mathbf{x}}})^{\mathbf{T}}\bar{\mathbf{H}}^{\mathbf{T}}\bar{\mathbf{H}}(\bar{\mathbf{x}}-\hat{\bar{\mathbf{x}}}) \le \mathbf{R}_{\mathbf{SD}}^{\mathbf{2}} \tag{4.13}$$

The SD method considers only the vectors inside a sphere defined by Equation (4.13). Figure 4.3 illustrates a sphere with the center of $\hat{\bar{\mathbf{x}}} = (\bar{\mathbf{H}}^{\mathbf{H}}\bar{\mathbf{H}})^{-1}\bar{\mathbf{H}}^{\mathbf{H}}\bar{\mathbf{y}}$ and radius of R_{SD}. In this example, this sphere includes four candidate vectors, one of which is the ML solution vector. We note that no vector outside the sphere can be the ML solution vector because their ML metric values are bigger than the ones inside the sphere (Yazdi, R. S., 2008.). If we were fortunate to choose the closest one among the four candidate vectors, we can reduce the radius in Equation (4.13) so that we may have a sphere within which a single vector remains. In other words, the ML solution vector is now contained in this sphere with a reduced radius, as illustrated in Figure 4.3(b).

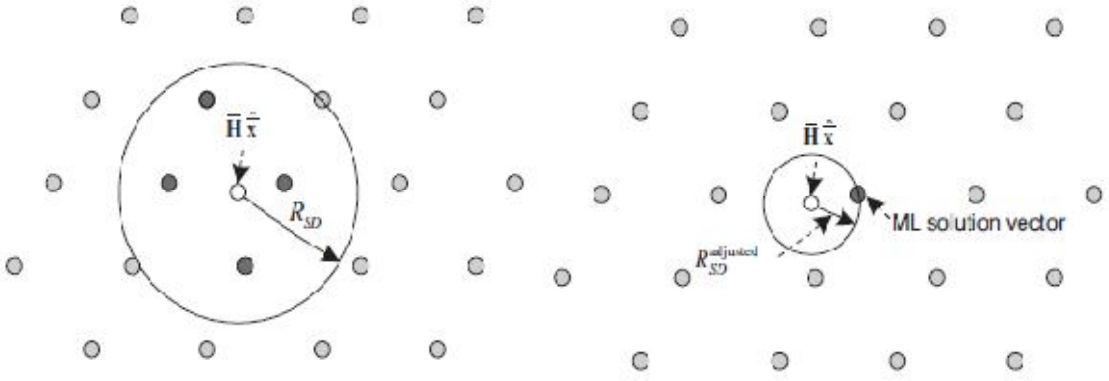

(a) Original sphere **(b) New sphere with the reduced radius**

Figure 4.3 Illustration of the sphere in sphere decoding. (Cho S. Y., 2012)

From QR decomposition of the real channel matrix $\bar{\mathbf{H}} = \mathbf{QR}$, when $N_T = N_R = 2$, the metric in equation can be expressed as (Cho S. Y., 2012)

$$\|\boldsymbol{R}(\bar{\boldsymbol{x}}-\hat{\boldsymbol{x}})\|^2 = \left\| \begin{bmatrix} r_{11} & r_{12} & r_{13} & r_{14} \\ 0 & r_{22} & r_{23} & r_{24} \\ 0 & 0 & r_{33} & r_{34} \\ 0 & 0 & 0 & r_{44} \end{bmatrix} \begin{bmatrix} \bar{x}_1-\hat{x}_1 \\ \bar{x}_2-\hat{x}_2 \\ \bar{x}_3-\hat{x}_3 \\ \bar{x}_4-\hat{x}_4 \end{bmatrix} \right\|^2$$

which, on applying sphere radius constraint R_{SD} will become:

$$|r_{44}(\bar{x}_4-\hat{x}_4)|^2 + |r_{33}(\bar{x}_3-\hat{x}_3) + r_{34}(\bar{x}_4-\hat{x}_4)|^2 + |r_{22}(\bar{x}_2-\hat{x}_2) + r_{23}(\bar{x}_3-\hat{x}_3) + r_{24}(\bar{x}_4-\hat{x}_4)|^2 + |r_{11}(\bar{x}_1-\hat{x}_1) + r_{12}(\bar{x}_2-\hat{x}_2) + r_{13}(\bar{x}_3-\hat{x}_3) + r_{14}(\bar{x}_4-\hat{x}_4)|^2 \leq R_{SD}^2 \quad (4.14)$$

4.6 Tree implementation of Sphere decoding algorithm

A QR factorization of the channel matrix (H = QR) allows transforming the system to an equivalent one that can be solved using a tree structure. Matrix Q is orthogonal, QQ^T = I, and matrix R can be decomposed into an upper triangular $2N_T \times 2N_T$ matrix, and a ($2N_R - 2N_T$) $\times$ $2N_T$ matrix of zeroes, now the problem can be equivalently expressed as (Cavallaro J. R., 2012).

$$\hat{s} = \arg\min_{s \epsilon C^{2N_T}} \{\|y' - Rx\|^2 \leq R_{SD}\} \quad (4.15)$$

In order to solve the above expression via a tree search, the following recursion is performed for i =$2N_T$, ... ,1:

$$T_i(X^{(i)}) = T_{i+1}(X^{i+1}) + \left|e_i X^{(i)}\right|^2 \quad (4.16)$$

where $e_i(X^{(i)}) = y_i' - \sum_{j=i}^{2n_T} r_{ij}x_j$, i denotes each tree level, $X^{(i)} = [x_i, x_{i+1}, \ldots, x_{2N_T}]$, $T_i X^{(i)}$ is the accumulated PartialEuclidean Distance (PED) up to level i, where T_{2N_T+1} +1($X^{(2N_T+1)}$) = 0, and $\left|e_i(X^{(i)})\right|^2$ is thedistance between levels i and i + 1 in the decoding tree, which will be represented as the branch weight (Radosavljevic P., 2012). Partial solutions are represented as nodes **n** and nodes are expanded in order to look for the ML solution or the closest lattice point. It is required to find the ML solution expanding as few nodes as possible in order to reduce the computational effort.

The tree will have as many levels as transmit antennas in the system (for complex constellations this number of levels will be doubled) and each node will have as many

children nodes as the constellation size (for complex constellations the size of the equivalent real. constellation will be considered instead). The search for the solution is performed in two levels, in each level branches with an accumulated PED higher than the sphere radius are discarded, resulting in less visited points (Varea, S. R., 2008).

Different tree search strategies have been proposed, but they can be classified into three main types of tree search: Breadth-First, Metric-First and Depth-First.

In the Breadth-First algorithms the tree is explored descending level by level up to the leaf nodes, every child in the same level has to be visited before starting to visit the following level. Figure 4.4 depicts the general idea behind Breadth-First algorithms. Breadth-first search has two major disadvantages: The first problem is associated with the need to choose an appropriate initial radius. I fit is chosen too small, no candidate vector symbol may meet the SC and the algorithm must be restarted with a larger radius (Choi J., 2012). If the radius is chosen too large, a considerable number of candidate vector symbols could meet the search constraint and the complexity will be high. The second problem is a consequence of the inability to determine a radius that guarantees that the number of nodes meeting the search constraint is low.

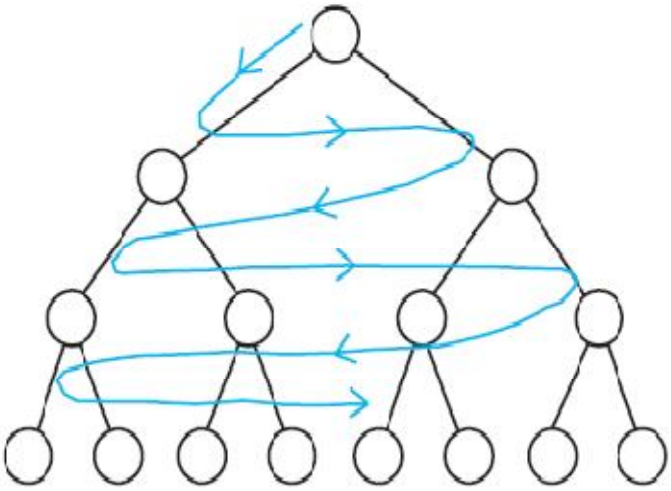

Figure 4.4: Decoding tree where a Breadth-First strategy is followed (Varea, S. R., 2008).

In metric first strategy, 2^M children nodes are evaluated at once and then the next mother node, which has the best metric among 2^M children nodes, is selected for next evaluation. Path histories and PEDs of evaluated nodes are stored into the memory except those of next mother node. In this case, it is expected that PED requires large number of multiplier and adder for evaluating 2^M children nodes at once and requires a large amount of memory. However it finds the ML solution fast. Figure 4.6 (b) illustrate the metric-first tree searching strategy. All children are evaluated at the first level then all children of mother node which has the minimum PED among nodes at the first layer is evaluated at the next step (Kim S. H., 2007).

In the Depth-First algorithms the tree is explored beginning from the root descending to the leaf nodes, but exploring every child node from left to right. Figure 4.5 makes clear this kind of search. The main advantages of a depth-first search over a breadth-first search are the reduced memory requirements and the fact that the depth-first algorithm quickly identifies candidate vector symbols that meet an initial search constraint (Choi J., 2012).

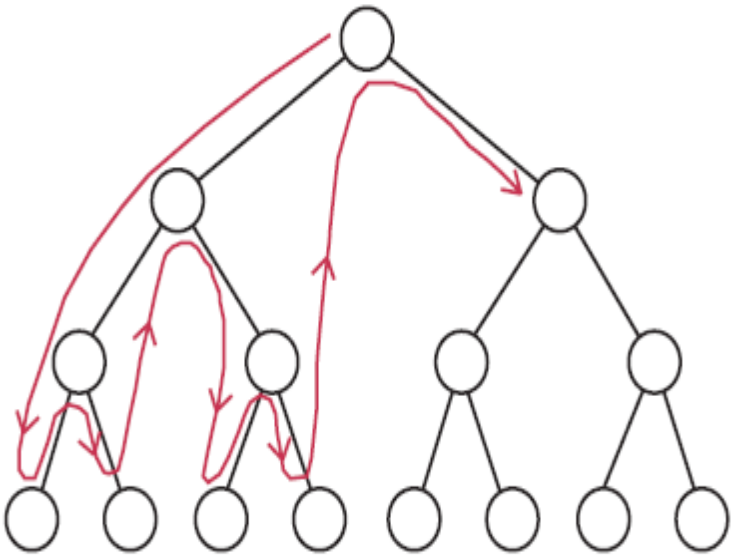

Figure 4.5: Decoding tree where a Depth-First strategy is followed (Varea, S. R., 2008).

Table 3 summarizes these three tree searching strategies.

Table 3: Tree search strategies used in Sphere decoding (Kim S. H., 2007).

	Depth First	**Metric First**	**Breath First**
Algorithm	Fincke and Phost	Schnorr-Euchner	K-Best
Path Extension (Forward)	One of the child of current node	All children of the current node whose PED is smallest among current children	All children from K survived nodes
Path Extension (Backward)	First untried node	All children of the nodes which has the smallest metric in the memory	-
# of paths to store	1	2^M per depth	K per depth
Pros.	The smallest storage size	The fastest searching speed	Deterministic throughput
Cons.	Searching speed is largely dependent on radius	The largest memory size	Performance degradation with small K

Proposed Sphere Decoding Algorithm for low radius.

Step 1: Inputs: H, symbolset(x), y, z, r

Step 2: Decompose channel matrix

[QR] = qr[H]

Step 3: No. of layers = Size[H]

Step 4: If Layer = 1, Else goto Step 6.

For symbol set x_i, calculate d

d = $Q^T y - R x_i$

Add previous distance d'

$d_{new} = d + d'$

Step 5: Check if all x_i checked?

If yes, d_{new} is the minimum noise and x_i is the optimal solution.

If no, I = i+1 check the next leaf node.

Step 6: if Layer ≠ 1

For symbol set x_i, calculate d

d = $Q^T y - Rx_i$

Add previous distance d'

$d_{new} = d + d'$

Check if $d_{new} < SphereRadius$

If yes, Layer=Layer + 1

If no, jump to the next sibling and continue.

Flowchart for Proposed Sphere Decoding Algorithm:

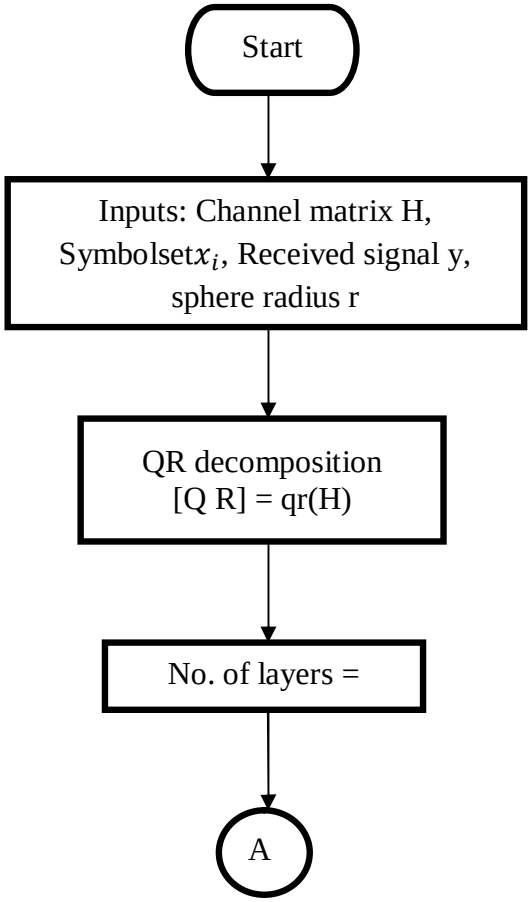

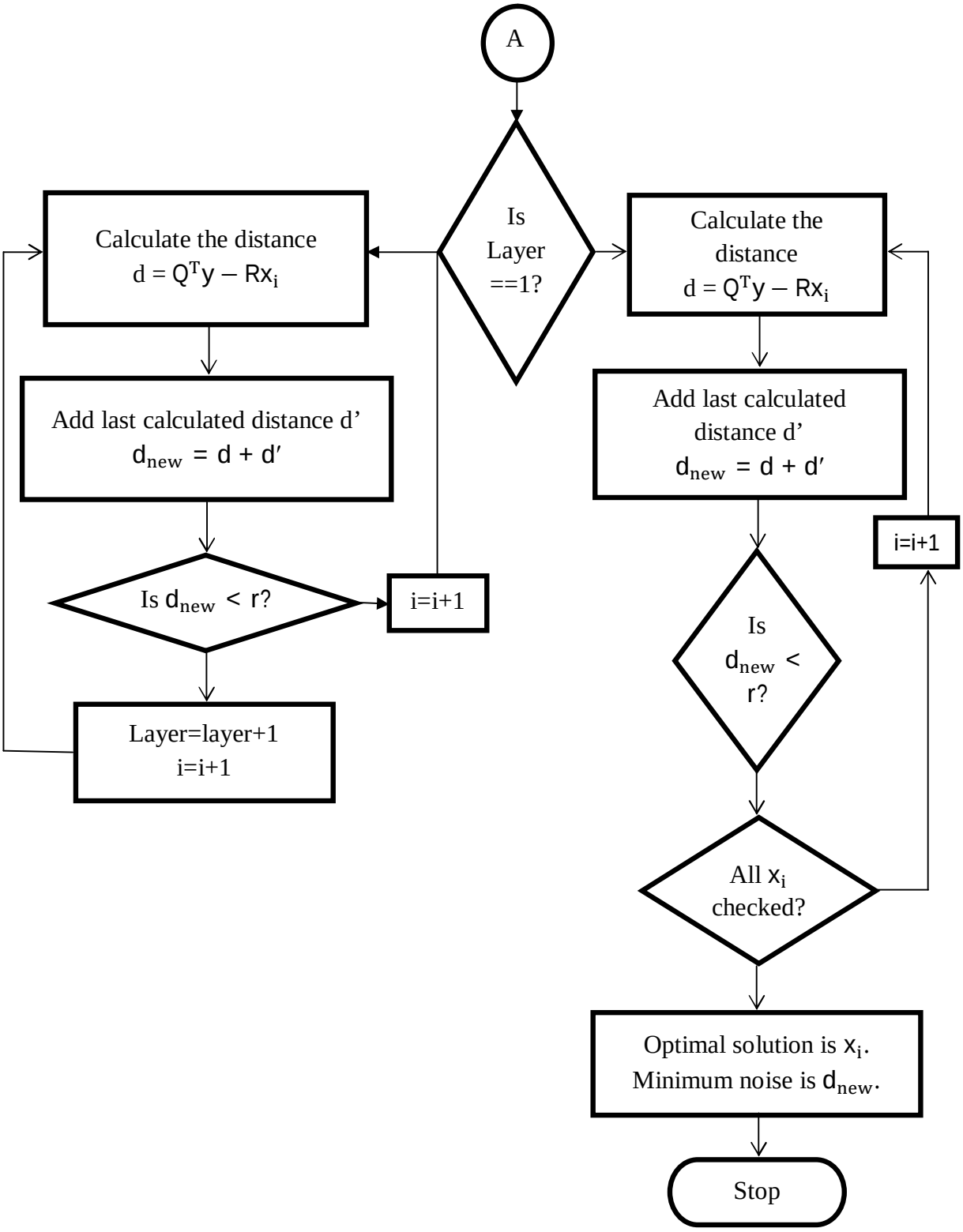
A
Is Layer ==1?
Calculate the distance $d = Q^T y - Rx_i$
Add last calculated distance d' $d_{new} = d + d'$
Is $d_{new} < r$?
i=i+1
Layer=layer+1 i=i+1
Calculate the distance $d = Q^T y - Rx_i$
Add last calculated distance d' $d_{new} = d + d'$
Is $d_{new} < r$?
i=i+1
All x_i checked?
Optimal solution is x_i. Minimum noise is d_{new}.
Stop

CHAPTER 5
RESULTS AND DICUSSION

For the current work we have modified the sphere decoding algorithm so as to achieve the following objectives:

1. Near optimal solution.
2. Less complexity.
3. Improved BER.

The modifications applied to the sphere decoding algorithm are:

1. The search is continued till a minimum number of leaf nodes are reached (i.e. one more than the number of leaf nodes associated with the parent node).
2. If no leaf node is found i.e. if the radius obtained for each leaf node is greater than the optimum radius, we jump to the next sibling.

For the simulation we have considered low radii sphere and the channel to be Rayleigh Flat fading Non Line of Sight (NLOS). Channel State Information (CSI) is assumed to be completely known at the receiver side. Antenna pairs of 2 x 2, 3 x 3 and 4 x 4, are simulated for 16-QAM, 32-QAM and 64-QAM. All these simulation parameters are tabulated in Table 4.

Table 4: Simulation parameters for sphere decoding algorithm.

Parameters		
Number of antennas		2,3,4
Modulation type		16-QAM, 32-QAM, 64-QAM
Fading channel		Rayleigh Flat fading Non Line of Sight (NLOS)
SNR range	2 x 2	0 – 30dB
	3 x 3	0 – 30dB
	4 x 4	0 – 30dB
CSI		Perfectly known
Channel coding		Uncoded
Symbols considered		2048

In Sphere decoding algorithm, the complexity of the algorithm mainly depends on the initial search radius, and is the only constraint that bounds the complexity. So in this work, firstly we have tried to find an optimal value of the search radius. For this we simulated 2 x 2 MIMO system with 16-QAM for 2048 different symbols. Signal-to-Noise Ratio (SNR) values were varied from 10 - 30 dB. We considered the sphere radius to be valid only if the leaf nodes enclosed by it are one more than the child nodes present. Considering low radii sphere we varied the sphere radius from 1 to 15 in steps of 1, and we repeated the same experiment 10 times. With all the results obtained from the 10 experiments, we took an average of all the obtained values of number of leaf nodes reached. This result is shown in figure 5.1. From this result the value of radius which reaches to one more than the child nodes present (i.e. 5 for the case of 2 x 2 MIMO system as it has 4 leaf nodes associated with every parent node) comes out to be 3. This sphere radius of 3 can be considered as the optimal value of the search radius as it neither visits too few nodes (decoding failure problem) nor visits too many nodes (Exhaustive search problem). Thus we have confined ourselves to a radius that saves us from high complexity, which occurs in both the cases of decoding failure problem as well as in exhaustive search problem.

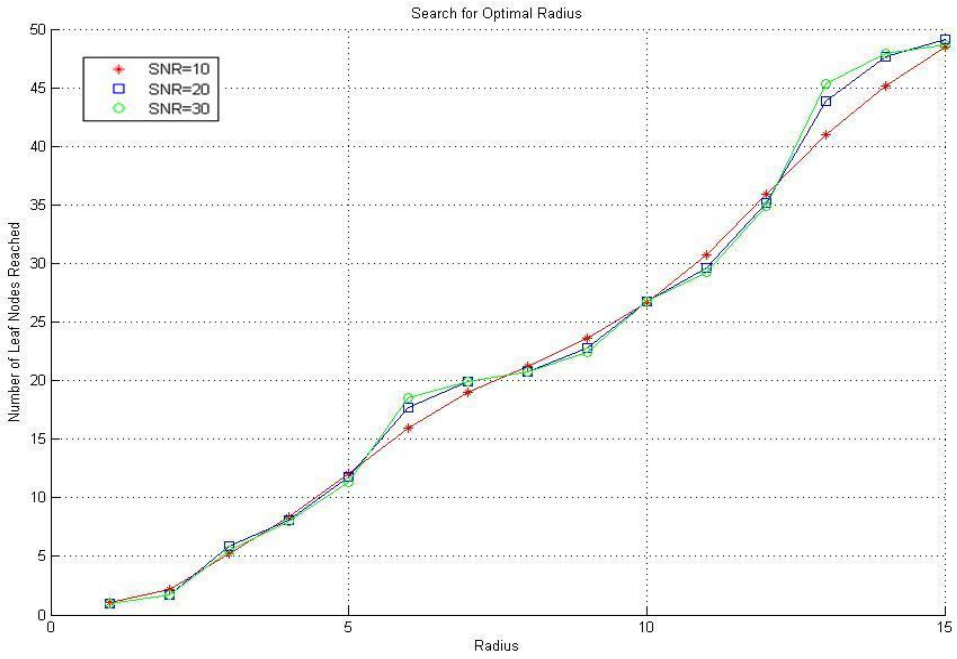

Figure 5.1: Number of leaf nodes reached for search radius of sphere decoding algorithm varying from 1 to 15 with SNR values of 10, 20 and 30.

Concluding 3 to be our optimal radius, we fixed *sphere radius* = 3 for the rest of the work. Now we tried to check for the Bit Error Rate (BER) for this optimal radius. We firstly simulated 16-QAM for 2 x 2 MIMO system with values of SNR varying from 1 to 30 in steps of 1. The result obtained can be seen in figure 5.2, it shows that the BER becomes zero at SNR = 6 and in the worst case BER is 2.25% at SNR =1.

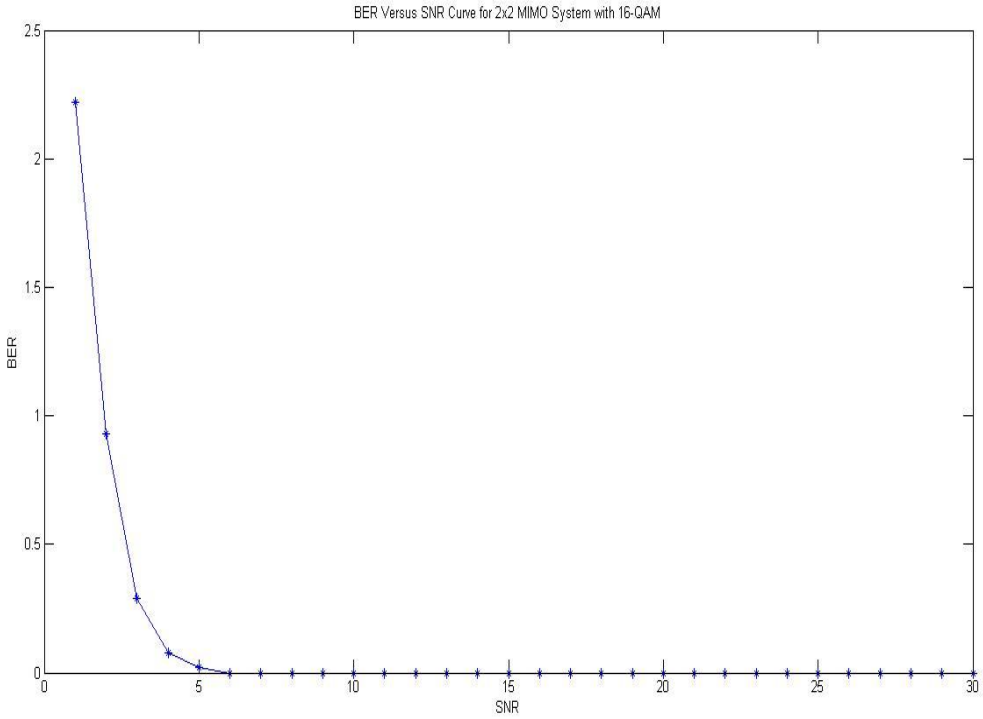

Figure 5.2: BER versus SNR curve for 2x2 MIMO system with 16-QAM.

Similarly we simulated 16-QAM for 3 x 3 MIMO system with values of SNR varying from 1 to 30 in steps of 1. The result obtained can be seen in figure 5.3, it shows that the BER becomes zero at SNR = 11 and in the worst case BER is 14% at SNR = 1.

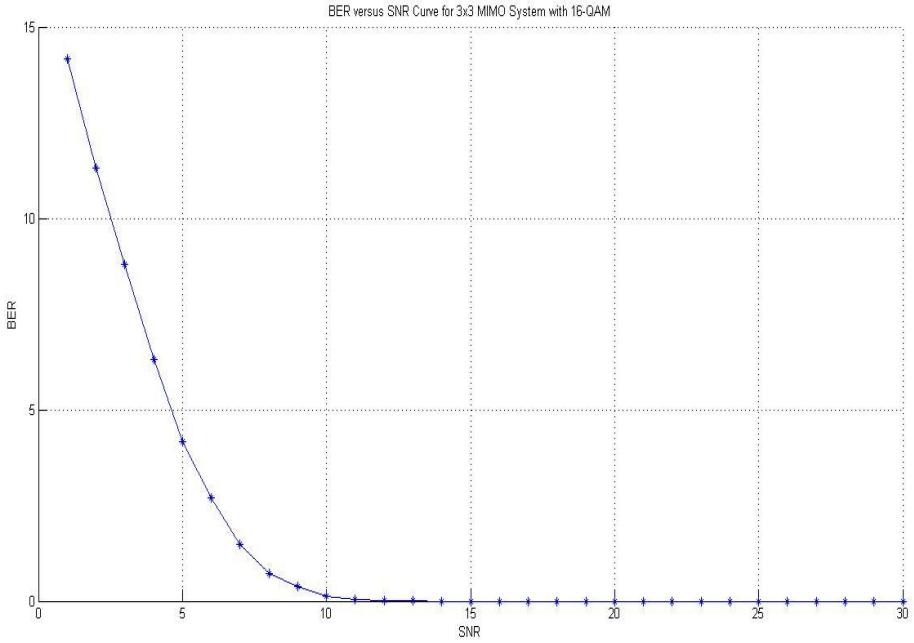

Figure 5.3: BER versus SNR curve for 3x3 MIMO system with 16-QAM.

Next we simulated 16-QAM for 4 x 4 MIMO system with values of SNR varying from 1 to 30 in steps of 1. The result obtained can be seen in figure 5.4, it shows that the BER becomes zero at SNR = 5 and in the worst case BER is 12% at SNR =1.

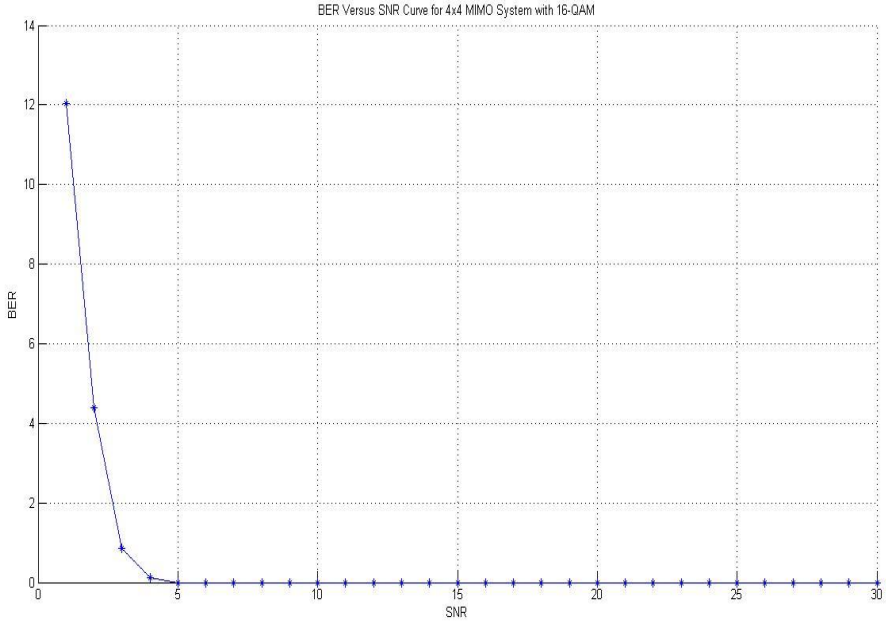

Figure 5.4: BER versus SNR curve for 4x4 MIMO system with 16-QAM.

With the same optimal radius found i.e. $R_{SD} = 3$, 32-QAM was simulated for 2 x 2, 3 x 3 and 4 x 4 MIMO systems to check for the BER. These obtained results are shown in figures 5.5, 5.6 and 5.7 respectively. For 32-QAM simulated with 2 x 2 MIMO system, BER became zero at SNR = 29 and in the worst case BER is found to be 77% at SNR = 1. For 32-QAM simulated with 3 x 3 MIMO system, BER becomes zero at SNR = 3 and in the worst case BER is found to be 0.1% at SNR =1.

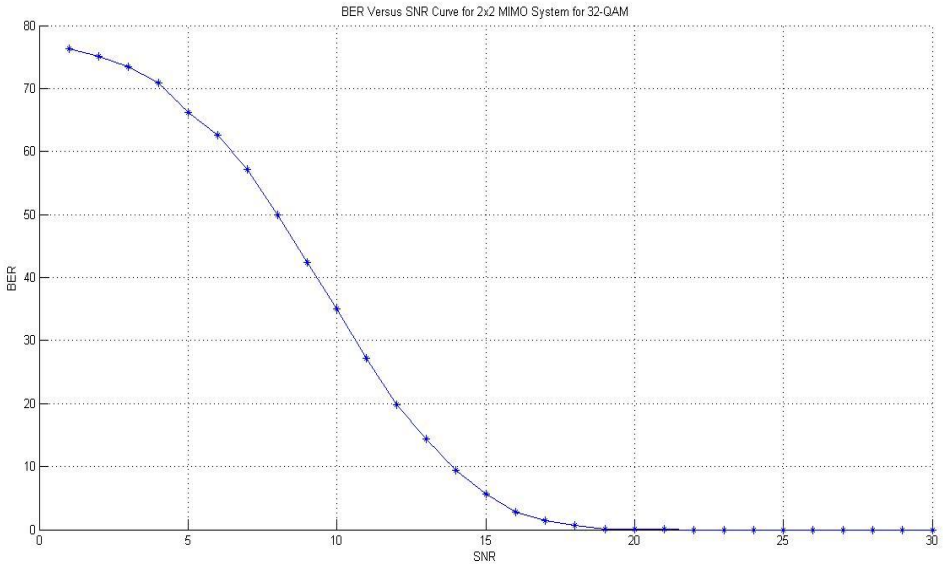

Figure 5.5: BER versus SNR curve for 2x2 MIMO system with 32-QAM.

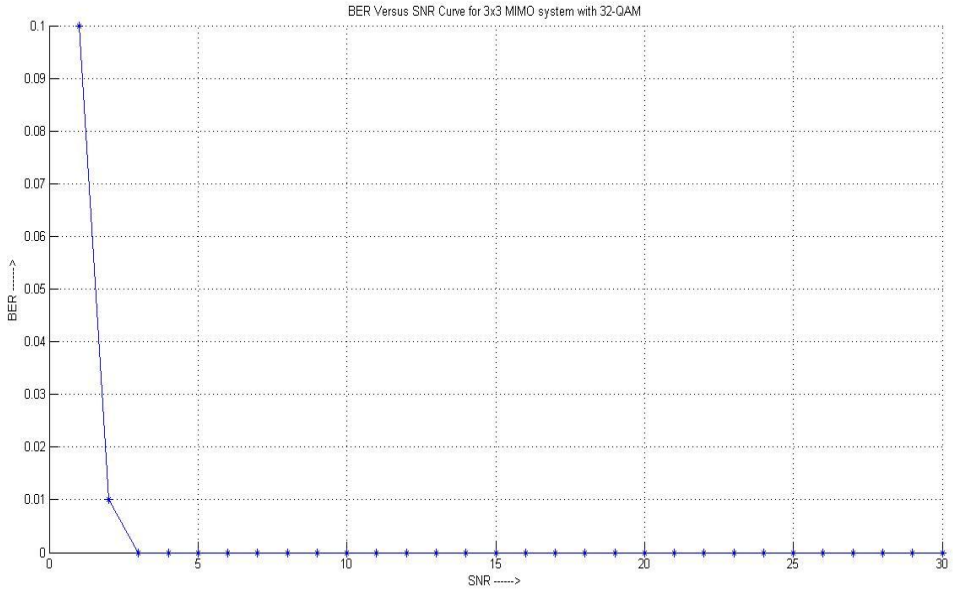

Figure 5.6: BER versus SNR curve for 3x3 MIMO system with 32-QAM.

For 32-QAM simulated with 4 x 4 MIMO system, BER becomes zero at SNR = 2 and in the worst case BER is found to be 0.01% at SNR =1.

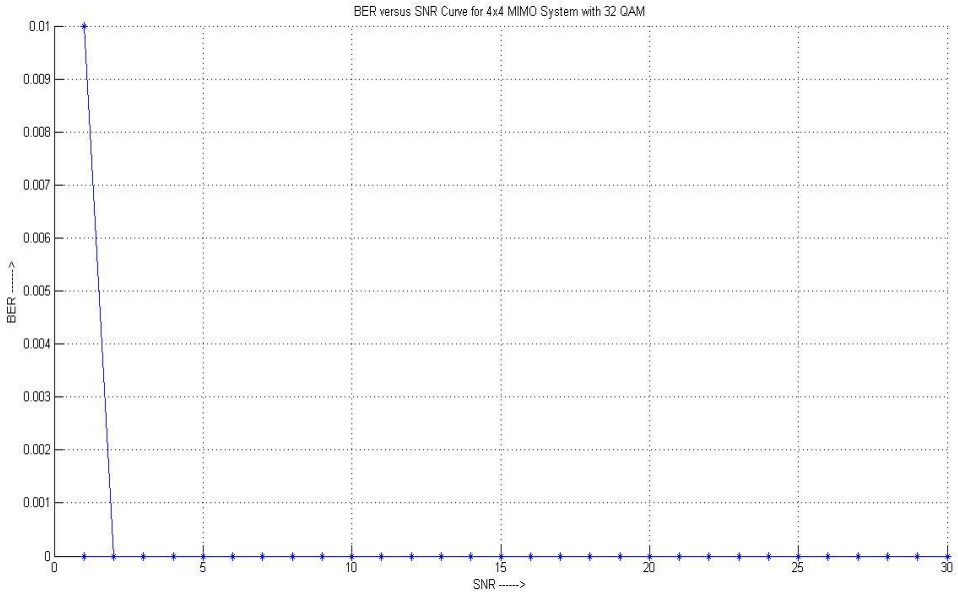

Figure 5.7: BER versus SNR curve for 4x4 MIMO system with 32-QAM.

Similarly the experiment was repeated for 64-QAM keeping optimal radius i.e. $R_{SD} = 3$. With 2 x 2 MIMO system simulated for 64-QAM, BER becomes zero at SNR = 7 and in the worst case BER is 8% at SNR =1, shown in figure 5.8.

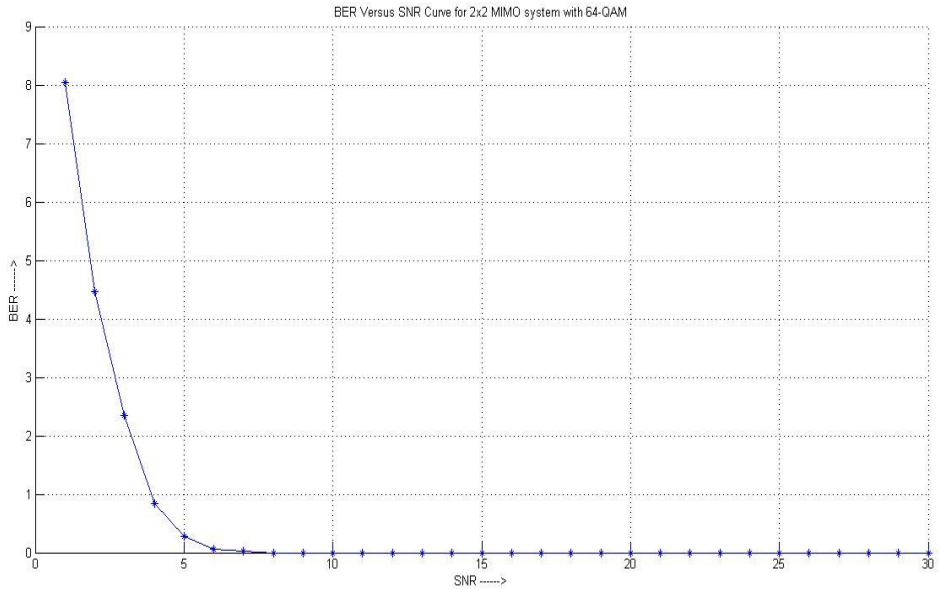

Figure 5.8: BER versus SNR curve for 2x2 MIMO system with 64-QAM.

With 3 x 3 MIMO system simulated for 64-QAM, BER becomes zero at SNR = 6 and in the worst case BER is 4.75% at SNR = 1, shown in figure 5.9.

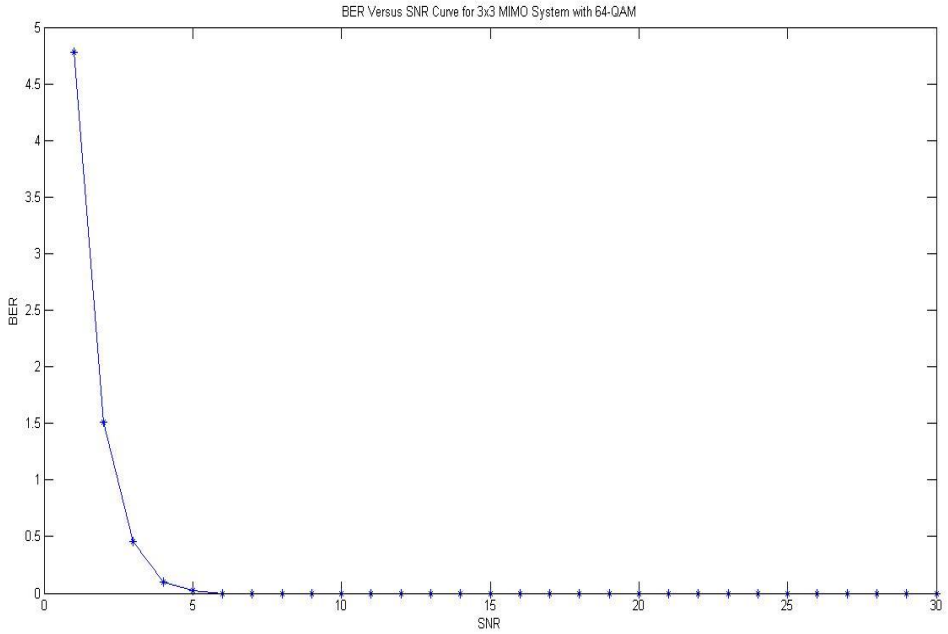

Figure 5.9: BER versus SNR curve for 3x3 MIMO system with 64-QAM.

With 4 x 4 MIMO system simulated for 64-QAM, BER becomes zero at SNR = 8 and in the worst case BER is 19% at SNR = 1, shown in figure 5.10.

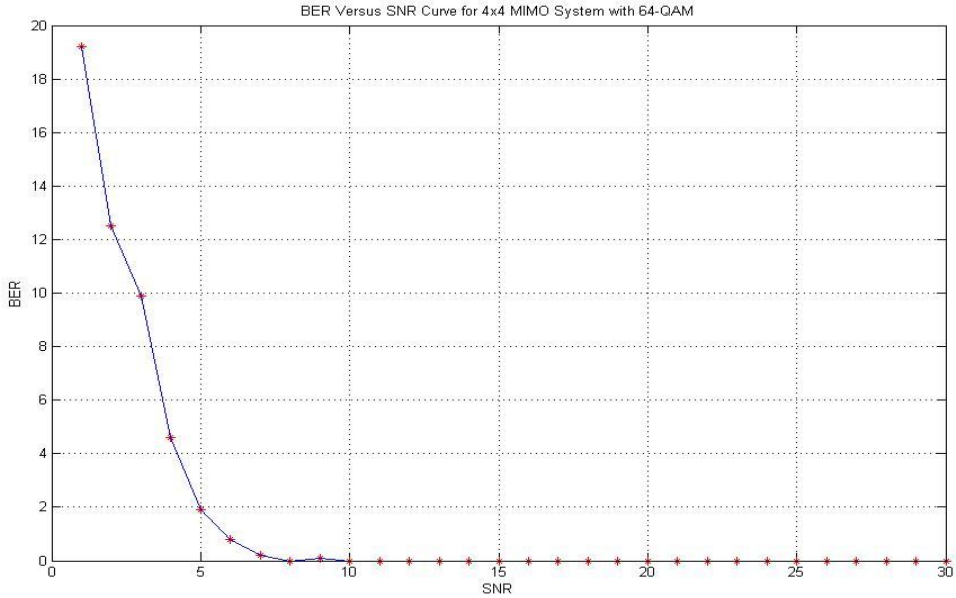

Figure 5.10: BER versus SNR curve for 4x4 MIMO system with 64-QAM.

Along with this work, we have also modified sphere decoding algorithm by the way we are obtaining the Q and R matrix in QR decomposition. Besides the conventional QR decomposition technique, we have also implemented Gram Schmitt orthogonalization QR decomposition, Household transformation QR decomposition, Givens rotation QR decomposition, and sorted QR decomposition techniques, and applied these decomposition techniques to our proposed sphere decoding algorithm. FLOPS in each QR decomposition technique varies, which varies the complexity of the decomposition technique, and hence of the algorithm associated with it.. Thus we are, by this experiment, trying to find out which of the above mentioned decomposition technique fits best with our proposed algorithm.

For this experiment we have again taken 2048 symbols, considered 2 x 2 MIMO system with 16-QAM, and we have just replaced the conventional QR decomposition technique by the above mentioned techniques, one-by-one, to check for the number of visited nodes. More the number of visited nodes, more will be the computations. Hence, we need to find a decomposition technique that reduces the number of visited nodes.

Results obtained (in the form of plot and histogram) for these decomposition techniques are shown in figures 5.11 to 5.15. From the results it can be clearly seen that Sorted QR decomposition technique visits 10 nodes while the rest of the decomposition techniques visit 11 nodes. Thus we have approximately 10% reduction in the number of visited nodes in this case.

Thus it can be concluded that using Sorted QR Decomposition along with the proposed sphere decoding algorithm achieves the objectives for the proposed work i.e. reduces complexity, gives near-optimal solution and improves BER.

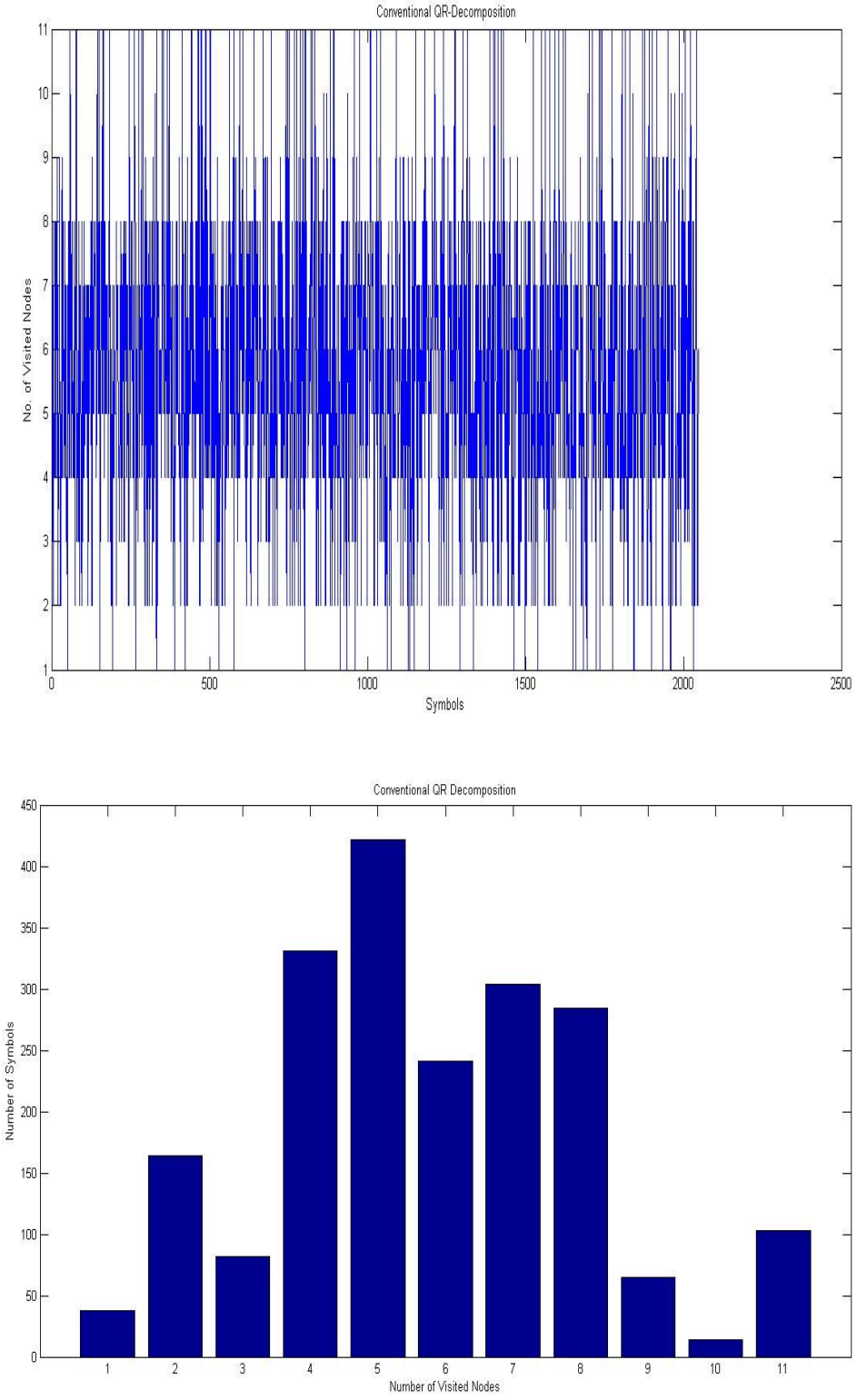

Figure 5.11: Number of visited nodes for Proposed Sphere Decoding algorithm with conventional QR Decomposition technique.

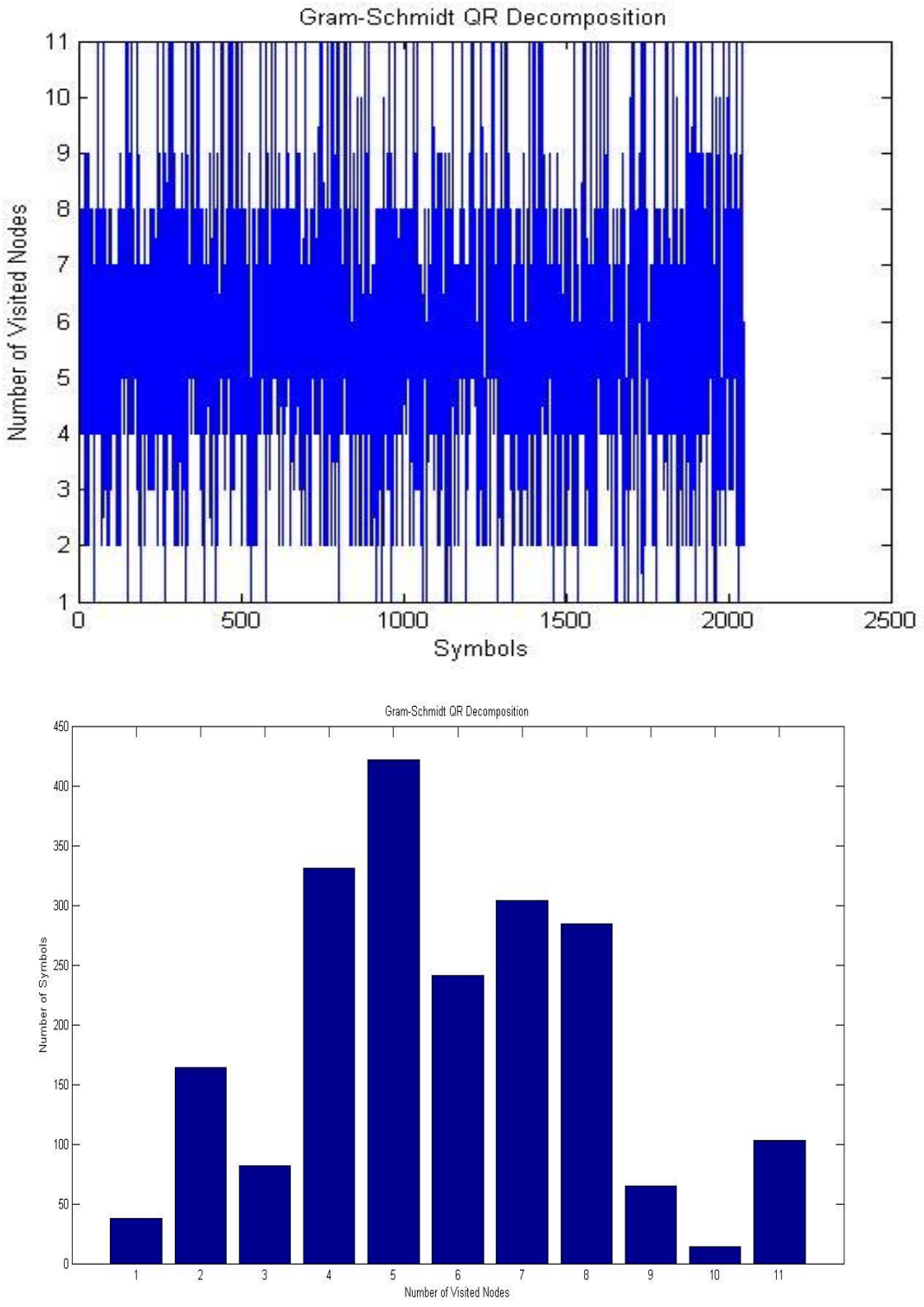

Figure 5.12: Number of visited nodes for Proposed Sphere Decoding algorithm with Gram-Schmidt QR Decomposition technique.

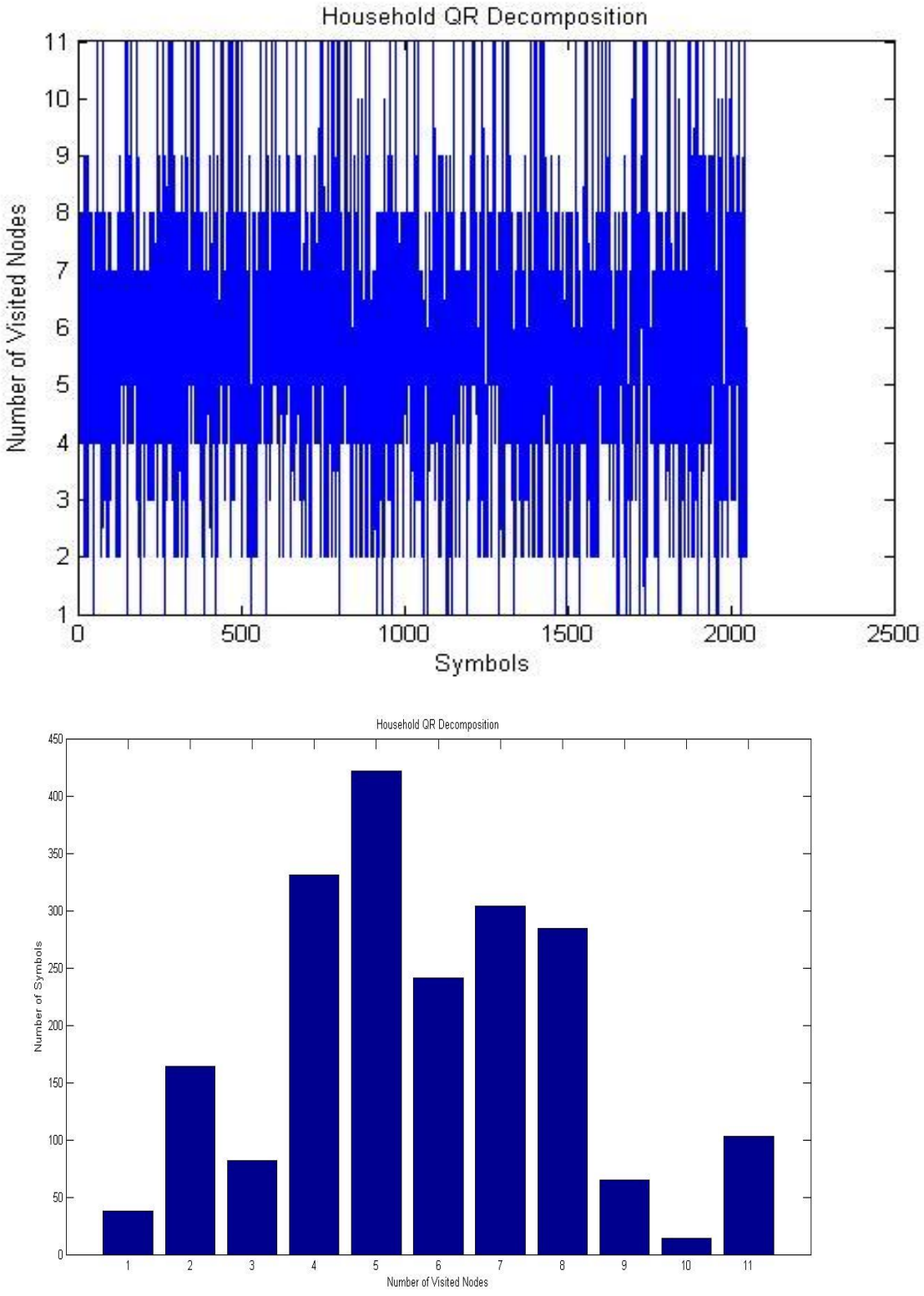

Figure 5.13: Number of visited nodes for Proposed Sphere Decoding algorithm with Household QR Decomposition technique.

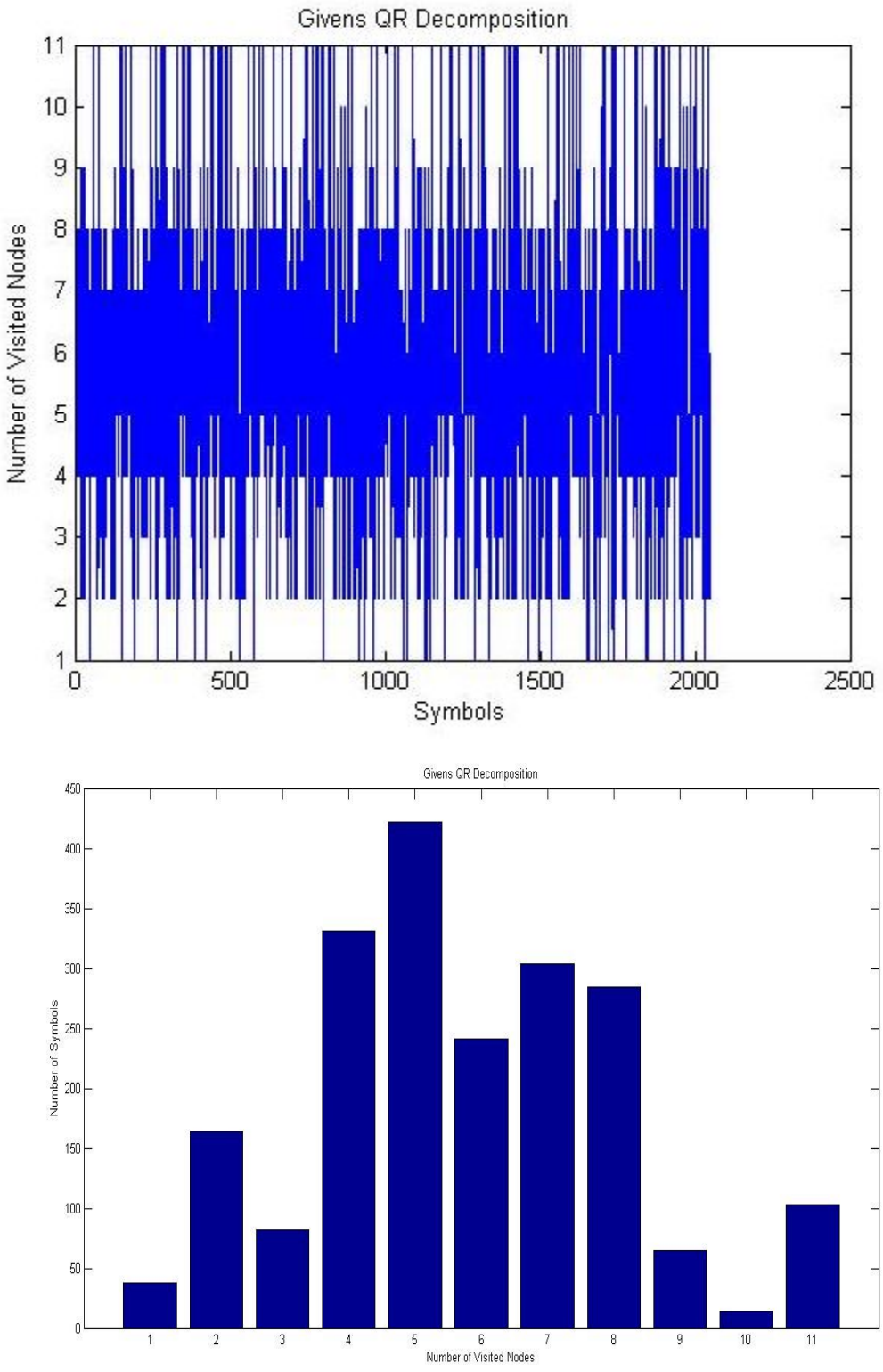

Figure 5.14: Number of visited nodes for Proposed Sphere Decoding algorithm with Givens QR Decomposition technique.

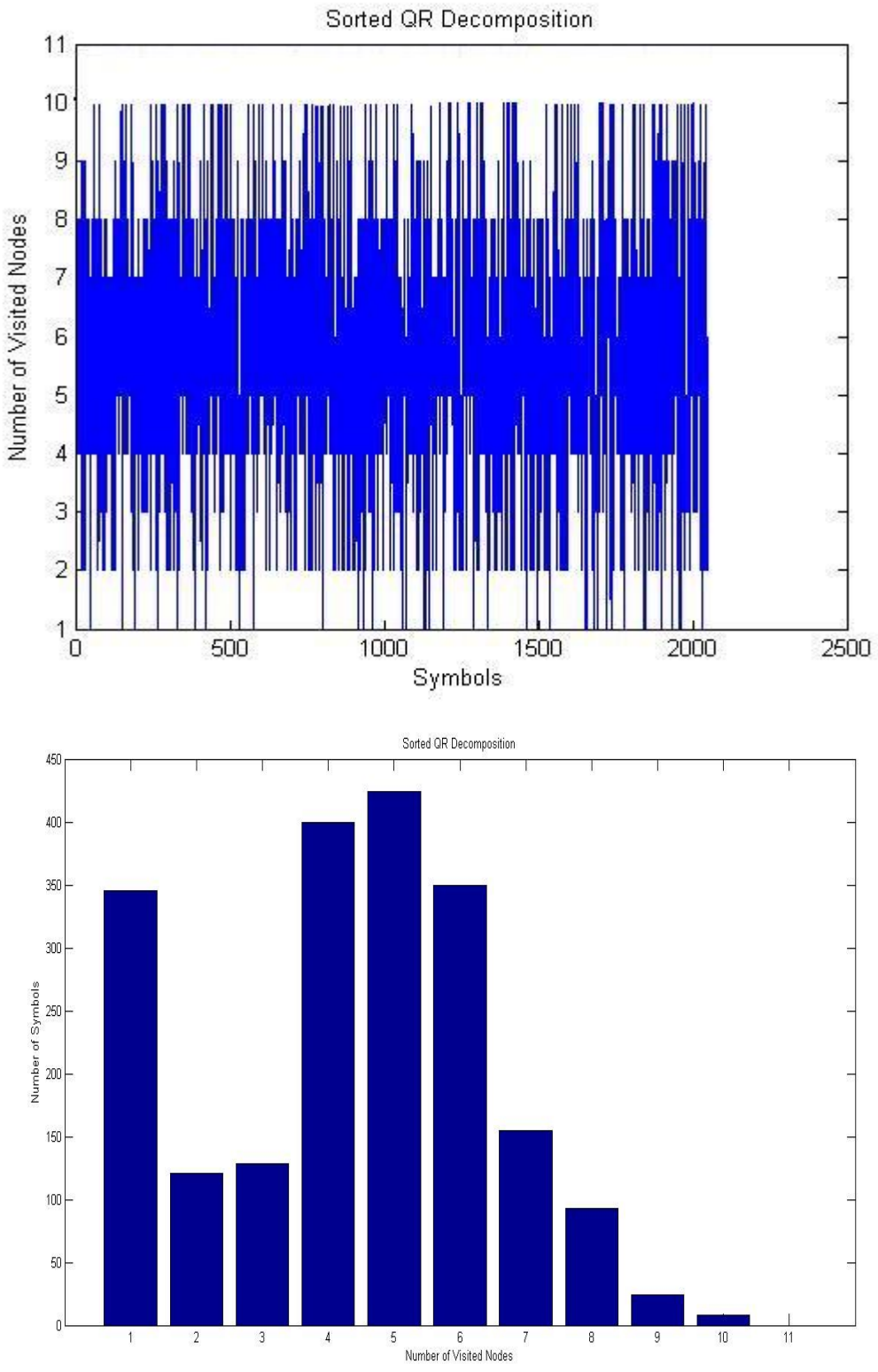

Figure 5.15: Number of visited nodes for Proposed Sphere Decoding algorithm with Sorted QR Decomposition technique.

Comparison of for Proposed algorithm with ML decoder.

Performance of the proposed algorithm is compared to ML decoder in terms of the number of nodes visited in reaching to an optimal solution. Since in case of ML detector we need to search through all the constellation points in order to reach to an optimal solution so the number of computations involved (addition, multiplication etc) and the number of visited nodes are much higher in value, and it goes on increasing with the constellation size as well as with the number of transmit antenna pairs used. In case of Proposed Sphere Decoding algorithm we confine ourselves to a sphere of definite radius which contains the optimal solution. With the sphere constraint known i.e. the radius of sphere within which we have to search for the optimal solution, reduces the number of nodes to be visited and hence the complexity of the system in terms of commutations.

Table 5 shows the difference in number of visited nodes for the proposed and ML detector. These results obtained through simulations are also shown in the figures 5.16, 5.17 and 5.18.

Table 5: Difference in number of visited nodes for the proposed and ML detector.

No. of visited nodes	**Proposed**	**ML**
2 x 2 MIMO 64-QAM	2081	4096
3 x 3 MIMO 64-QAM	10406	262144
4 x 4 MIMO 64-QAM	20802	16777216

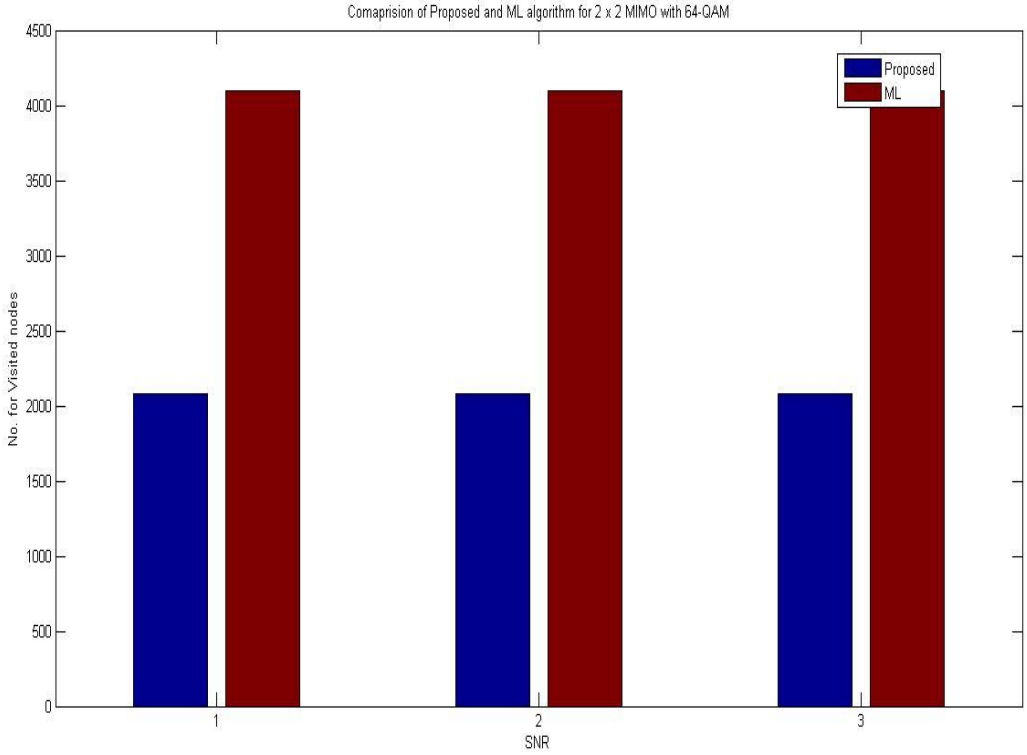

Figure 5.16: Number of visited nodes for Proposed and ML decoder for 2 x 2 MIMO system with 64 QAM.

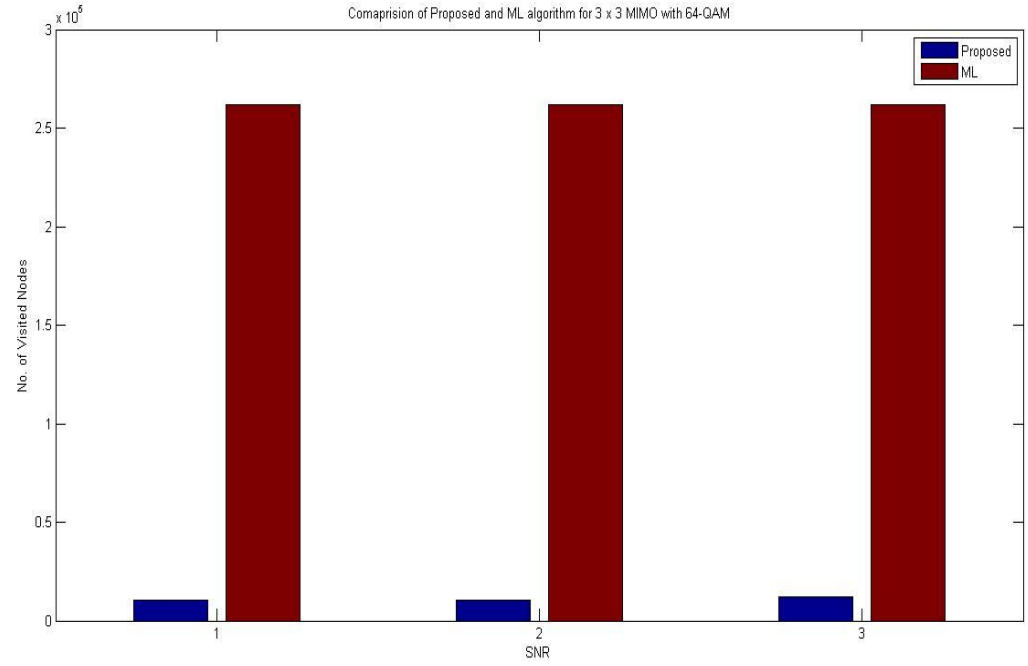

Figure 5.17: Number of visited nodes for Proposed and ML decoder for 3 x 3 MIMO system with 64 QAM.

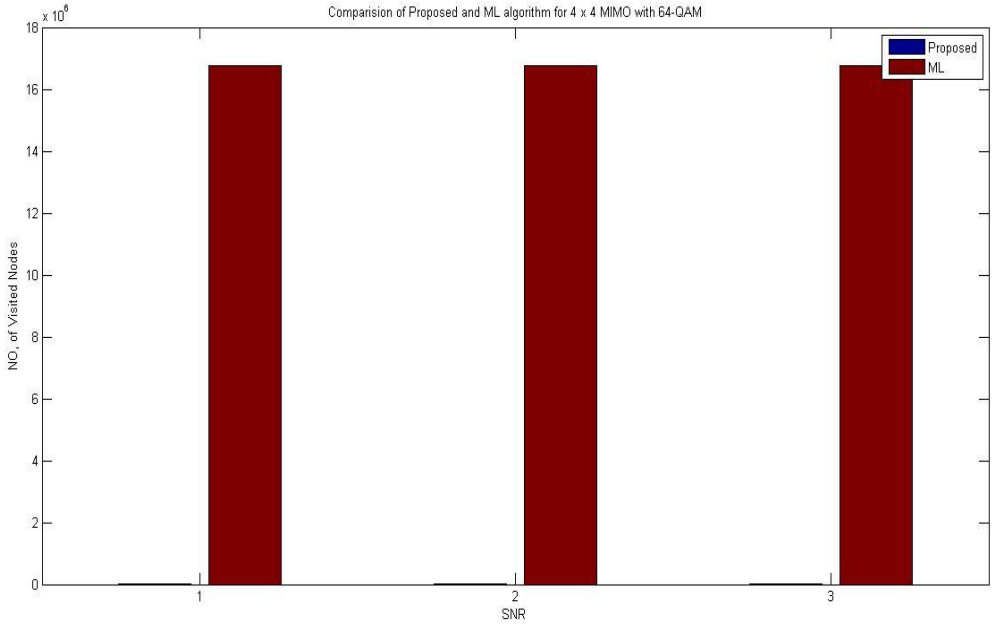

Figure 5.18: Number of visited nodes for Proposed and ML decoder for 4 x 4 MIMO system with 64 QAM.

CHAPTER 6
SUMMARY

In the present work we had an in-depth study of sphere decoding algorithm and its modifications. Every individual has tried his own way to make the MIMO receiver-end a little less complex. The major constraint that comes into picture is the initial sphere radius to start with. Inspired by this we have modified the sphere decoding algorithm and conducted an experiment in which we varied the sphere radius and checked for the number of leaf nodes reached. Through the obtained simulation results we found that 3 is the favorable search radius that neither visits too many nodes nor it leads to decoding failure problem, which occurs when there exists no candidate node inside the search radius.

Then, with our concluded optimal search radius, we simulated 16-QAM, 32-QAM, and 64-QAM for 2 x 2, 3 x 3 and 4 x 4 MIMO systems. For all these simulations we obtained the results in the form of BER versus SNR curves. While simulating we did not encountered any decoding failure problem, also the BER values obtained were in permissible limits.

Lastly, modification was applied on the QR decomposition technique. We implemented Gram-Schmidt orthogonalization, Household transformation, Givens rotation and Sorted QR decomposition to obtain Q and R matrices. With the results obtained, it is found that Sorted QR Decomposition technique reduces the number of visited nodes by 20-25%, hence it best fits with the proposed algorithm.

The current work can be extended in future by adopting lattice reduction based sphere decoding, which further improves the performance.

Literature Cited

Amiri, K., Dick, C., Rao, R., Cavallaro, J.R., 2008. Novel Sort-Free Detector with Modified Real-Valued Decomposition (M-RVD) Ordering in MIMO Systems. *IEEE transactions on signal processing* **8**, 4244-2324.

Azzam, L., Ayanoglu, E., 2007. Reduced Complexity Sphere Decoding for Square QAM via a New Lattice Representation. *IEEE transactions on signal processing* **7** : 4242-4246.

Bai, L., Choi, J., 2012. Low Complexity MIMO Detection, Springer.

Biglieri, E., 2007. MIMO Wireless Communications, Cambridge University Press.

Chan, A.M., Lee, I., 2002. A New Reduced-Complexity Sphere Decoder for Multiple Antenna System, *IEEE* ISSN: 0-7803-7400-2/**02**

Cho, S.Y., Kim, J., Yang, W.Y., Kang, C., 2012. MIMO-OFDM wireless communication with MATLAB. Wiley Publications.

Damen, M.O., Gamal, H.E., Caire, G., 2003. On Maximum-Likelihood Detection and the Search for the Closest Lattice Point. *IEEE Trans. Inform. Theory* **49**.

Fessler, J.A., Hero, A.O., 1994. Space-alternating generalized EM algorithm, *IEEE Trans. Signal Processing* **42** : 2664–2677.

Fincke, U., Pohst, M., 1985. Improved methods for calculating vectors of short length in a lattice, including a complexity analysis, *Mathematics of Computation* **44** : 463–471.

Foschini, G.J., Gans, M.J., 1998. On limits of wireless communications in a fading environment when using multiple antennas. *Wireless Personal Communications* **6** : 311– 335.

Goldsmith, A., 2005. Wireless Communications, Cambridge University Press.

Guo, Z., Nilsson, P., 2004. Reduced Complexity Schnorr–Euchner Decoding Algorithms for Systems. *IEEE Communications Letters* **8**.

Han, S., Cui, T., Tellambura, C., 2012. Improved K-Best Sphere Detection for Uncoded and Coded MIMO Systems. *IEEE wireless communications letters* **1**, 472-475.

Hassibi, B., Vikalo, H., 2005. On the Sphere-Decoding Algorithm-I : Expected Complexity. *IEEE transactions on signal processing* **53**, 2806-2818.

Huang, C., Wu, C., Lee, T., 2011. Geometry based efficient decoding algorithms forunder determined MIMO systems. *IEEE 12th International Workshop on Signal Processing Advances in Wireless Communications*.

Jafar, S., 2005. Degrees of freedom in distributed MIMO communications. *IEEE Communication Theory Workshop*.

Jald´en, J., Ottersten, B., 2005. On the Limits of Sphere Decoding, *International Symposium on Information Theory*.

Kannan, R., 1983. Improved algorithms on integer programming and related lattice problems. *Proceedings of the 15th Annual ACM Symposium on Theory of Computing* : 193–206.

Kermoal, J.P., Schumacher, L., Mogensen, P. E., Pedersen, K.I., 2000. Experimental investigation of correlation properties of MIMO radio channels for indoor picocell scenarios. *Proc. IEEE VTC* **1** : 14–21.

Ketonen, J., Juntti, M., Cavallaro, J. R., 2010. Performance—Complexity Comparison of Receivers for a LTE MIMO System. *IEEE transactions on signal processing* **8** : 3360-3372.

Khan, A.A., 2008. Symbol Detection Techniques in a Spatial Multiplexing System, PhD thesis submitted to Department of Electrical and Computer Engineering, University of Engineering and Technology, Taxila.

Kim, S.H., 2007. Study of Sphere Decoder Architecture for MIMO wireless communication systems. Master's thesis submitted to KAIST Information and Communications University.

Lagarias, J.C., Lenstra, H.W., Schnorr C.P., 1990. Korkin-Zolotarev bases and successive minima of a lattice and its reciprocal lattice. *Combinatorica* **10** : 333–348.

Liang, H., Chung, W., Zhang, H., Kuo, S., 2012. A Parallel Processing Algorithm for Schnorr-Euchner Sphere Decoder. *IEEE Wireless Communications & Networking Conference: PHY and Fundamentals*.

Ling, C., Mow, W.H., Gan, L., 2010. Dual-Lattice Ordering and Partial Lattice Reduction for SIC-Based MIMO Detection. *Submission to IEEE Journal on selected topics in Signal Processing.*

Lathi, B.P. 1998. Modern Digital and Analog Communication Systems. Oxford University Press.

Mo, M., He, C., Yang, F., 2011. The Analyzation on the Performance and Complexity of Sphere Decoding Algorithms. *Crown* ISSN: 978-1-4244-6252-0/**11.**

Myllylä, M., Juntti, M., Cavallaro, J.R., 2008. The Effect of Preprocessing to the Complexity of List Sphere Detector Algorithms. *WPMC Proceedings*.

Myllylä, M., Juntti, M., Cavallaro, J.R., 2008. Implementation and Complexity Analysis of List Sphere Detector for MIMO systems. *IEEE transactions on signal processing* **8** : 4244-2941.

Myllylä, M., Hintikka, J., Cavallaro, J.R., Juntti, M., 2005. Complexity Analysis of MMSE Detector Architectures for MIMO Systems. *IEEE transactions on signal processing* **5** : 4244-4251.

Myllylä, M., Silvola, P., Juntti, M., Cavallaro, J.R., 2006. Comparison of two novel list sphere detector algorithms for MIMO systems. *17th Annual IEEE International Symposium on Personal, Indoor and Mobile Radio Communications (PIMRC'06)*.

Pohst, M., 1981. On the computation of lattice vectors of minimal length, successive minima and reduced bases with applications, *ACM SIGSAM Bulletin* **15** : 37–44.

Radosavljevic, P., Kim, K.J., Shen, H., Cavallaro, J.R., 2012. Parallel Searching-Based Sphere Detector for MIMO Downlink OFDM Systems. *IEEE transactions on signal processing* **60** : 3240-3252.

Rappaport, T.S., 2009. Wireless Communication: Principles and Practice, Prentice Hall.

Shi-Ping, Li., Long, W., Fang-Chao, C., 2012. Ordered Sphere Decoding Detection Algorithm for MIMO Systems. *24th Chinese Control and Decision Conference (CCDC)* : 3322-3325.

Stojnic, M., Vikalo, H., Hassibi, B., 2008. Speeding up the Sphere Decoder With H^{∞} and SDP Inspired Lower Bounds. *IEEE transactions on signal processing* **56** : 712-726.

Sun, Y., Cavallaro, J.R., 2012. Trellis-Search Based Soft-Input Soft-Output MIMO Detector: Algorithm and VLSI Architecture. *IEEE transactions on signal processing* **60** : 2617-2627.

Sun, Y., Cavallaro, J.R., 2010. Low-complexity and high-performance soft MIMO detection based on distributed M-algorithm through trellis-diagram. *IEEE transactions on signal processing* **10** : 4244-4296.

Sun, Y., Cavallaro, J.R., 2012. High-Throughput Soft-Output MIMO Detector Based on Path-Preserving Trellis-Search Algorithm. *IEEE transactions on very large scale integration (VLSI) systems* **20** : 1235-1247.

Telatar, I.E., 1999. Capacity of multi-antenna Gaussian channels. *European Trans. Tel.* **10 :** 585–595.

Varea, S.R., 2008. Efficient detection algorithms for Multiple-Input Multiple-Output (MIMO) Systems. PhD thesis.

Viterbo, E., Boutros, J., 1999. A universal lattice code decoder for fading channels. *IEEE Transactions on Information Theory* **45** : 1639–1642.

Wu, M., Dick, C., Sun, Y., Cavallaro, J.R., 2011. Improving MIMO Sphere Detection Through Antenna Detection Order Scheduling. *Proceedings of the SDR 11 Technical Conference and Product Exposition*.

Yazdi, R.S., Kwasniewski, T., 2008. Low Complexity Sphere Decoding Algorithms. *IEEE* ISSN : 978-1-4244-2489-4/**08.**